The FEBS Journal

FEBS PRESS science publishing by scientists

Unsaturated fatty acids augment protein transport via the SecA:SecYEG translocon

Michael Kamel[1], Maryna Löwe[1], Stephan Schott-Verdugo[2,3], Holger Gohlke[2,3] and Alexej Kedrov[1]

1 Synthetic Membrane Systems, Institute for Biochemistry, Heinrich Heine University Düsseldorf, Germany
2 Institute for Pharmaceutical and Medicinal Chemistry, Heinrich Heine University Düsseldorf, Germany
3 John von Neumann Institute for Computing (NIC), Jülich Supercomputing Centre (JSC), Institute of Biological Information Processing (IBI-7: Structural Bioinformatics), and Institute of Bio- and Geosciences (IBG-4: Bioinformatics), Forschungszentrum Jülich GmbH, Germany

Keywords
membrane organization; protein:lipid interactions; translocase

Correspondence
A. Kedrov, Synthetic Membrane Systems, Institute for Biochemistry, Heinrich Heine University Düsseldorf, Universitätsstraße 1, 40225 Düsseldorf, Germany
Tel: 0049 211 81 13271
E-mail: Kedrov@hhu.de
and
H. Gohlke, Institute for Pharmaceutical and Medicinal Chemistry, Heinrich Heine University Düsseldorf, Universitätsstraße 1, 40225 Düsseldorf, Germany
Tel. 0049 211 8113662
E-mail: hogoh001@hhu.de

(Received 9 April 2021, revised 1 July 2021, accepted 23 July 2021)

doi:10.1111/febs.16140

The translocon SecYEG and the associated ATPase SecA form the primary protein secretion system in the cytoplasmic membrane of bacteria. The secretion is essentially dependent on the surrounding lipids, but the mechanistic understanding of their role in SecA : SecYEG activity is sparse. Here, we reveal that the unsaturated fatty acids (UFAs) of the membrane phospholipids, including tetraoleoyl-cardiolipin, stimulate SecA : SecYEG-mediated protein translocation up to ten-fold. Biophysical analysis and molecular dynamics simulations show that UFAs increase the area per lipid and cause loose packing of lipid head groups, where the N-terminal amphipathic helix of SecA docks. While UFAs do not affect the translocon folding, they promote SecA binding to the membrane, and the effect is enhanced up to fivefold at elevated ionic strength. Tight SecA : lipid interactions convert into the augmented translocation. Our results identify the fatty acid structure as a notable factor in SecA : SecYEG activity, which may be crucial for protein secretion in bacteria, which actively change their membrane composition in response to their habitat.

Abbreviations
ATPase, adenosine triphosphatase; bis(PO)CL, 1′,3′-bis[1-palmitoyl-2-oleoyl-sn-glycero-3-phospho]-glycerol; CL, cardiolipin; DDM, n-dodecyl-β-D-maltoside; DHFR, dihydrofolate reductase; DOPC, 1,2-dioleoyl-sn-glycero-3-phosphatidylcholine; DOPE, 1,2-dioleoyl-sn-glycero-3-phosphatidylethanolamine; DOPG, 1,2-dioleoyl-sn-glycero-3-phospho-(1′-rac-glycerol); DPH, 1,6-Diphenyl-1,3,5- hexatriene; DPPC, 1,2-dipalmitoyl-sn-glycero-3-phosphocholine; DPPG, 1,2-dipalmitoyl-sn-glycero-3-phospho-(1′-rac-glycerol); DSF, differential scanning fluorimetry; *E.* coli, Escherichia coli; FM, fluorescein-5-maleimide; FRET, Förster's resonance energy transfer; KCl, potassium chloride; KOAc, Potassium acetate; KOH, potassium hydroxide; MD, molecular dynamics; $Mg(OAc)_2$, magnesium acetate; $MgCl_2$, magnesium chloride; NaOH, sodium hydroxide; Ni^{2+}-NTA, nickel-nitrilotriacetic acid; PC, phosphatidylcholine; PDB, protein data bank; PE, phosphatidylethanolamine; PG, phosphatidylglycerol; POPC, 1-palmitoyl-2-oleoyl-glycero-3-phosphatidylcholine; POPE, 1-palmitoyl-2-oleoyl-glycero-3-phosphatidylethanolamine; POPG, 1-palmitoyl-2-oleoyl-sn-glycero-3-phosphatidyl-(1′-rac-glycerol); QCM-D, quartz crystal microbalance with dissipation; SDS/PAGE, sodium dodecyl sulfate/polyacrylamide gel electrophoresis; SLB, supported lipid bilayer; SPR, surface Plasmon resonance; TCA, trichloroacetic acid; TCEP, tris(2-carboxyethyl) phosphine; TOCL, 1′,3′-bis[1,2-dioleoyl-sn-glycero-3-phospho]-glycerol; Tris/HCl, tris (hydroxymethyl) aminomethane hydrochloride; UFA, unsaturated fatty acid.

Introduction

Protein transport across the cytoplasmic bacterial membrane is an essential step in biogenesis of cell envelope and secretory proteins [1]. Most of these proteins cross the membrane post-translationally as unfolded precursors (preproteins). The preproteins with cleavable N-terminal hydrophobic signal sequences are picked up by holdase chaperones, such as SecB, and delivered to the Sec machinery (Fig. 1A). The core of the Sec machinery consists of the heterotrimeric membrane-embedded channel, or *translocon*, SecYEG, and the membrane-associated ATPase SecA. The translocon builds a narrow transmembrane conduit for the unfolded preproteins, and it is primed by insertion of the signal sequence at the translocon : lipid interface. The activity of the SecYEG-bound ATPase SecA provides the energy for directional transport of the preprotein through the translocon [2].

The crucial role of the lipid environment for Sec-mediated protein transport has been generally acknowledged, with a primary focus on electrostatic interactions at the membrane interface [3–6]. The anionic lipids, mainly phosphatidylglycerol (PG) and cardiolipin (CL), mediate anchoring of SecA at the membrane interface even in the absence of SecYEG [3,7], as they interact with the basic residues within the N-terminal helix of the ATPase. In contrast to the lipid head groups, only limited insights on the effect of the constituting fatty acids are available. Initial *in vitro* experiments revealed that dioleoyl-phosphatidylethanolamine (DOPE) stimulates preprotein translocation [5]. The effect was attributed to the conical shape of DOPE molecules built of two mono-unsaturated fatty acids (UFAs) and the small head group, but the mechanistic explanation of the stimulation remained obscure. This limited knowledge contrasts the essential complexity of cellular membranes, where the diversity of fatty acids that constitute lipids arises from variations in their length and the unsaturation level. Furthermore, cells regulate the UFA content in response to changing environmental factors, the habitat style and the growth phase, so the ratio of UFAs to saturated fatty acids in the inner membrane of *E. coli* changes from 1 : 1 to 2 : 1 when the growth temperature is reduced to 17 °C [8,9]. Several membrane-associated protein complexes in bacteria and eukaryotes appear to be sensitive to the UFA content, having an effect on signalling reactions, protein folding and degradation [10–12].

Here, we demonstrate for the first time that changes in the UFA content in phospholipids have a notable effect on SecA : SecYEG-mediated protein translocation. Increasing the *cis*-UFA content from 50 to 100 mol % within the fluid phase membrane leads to a fivefold increase in the translocon activity. Biophysical analysis and all-atom molecular dynamics simulations show that the structure of the fatty acids does not affect SecYEG stability, but UFAs determine a loosely packed membrane interface and facilitate apolar SecA : lipid interactions. The stimulated association of the ATPase with the lipid membrane leads to the augmented activity of the SecA : SecYEG complex. We further demonstrate that the UFA-enriched tetraoleoyl-CL stimulates the translocation up to ten-fold, and the stimulation does not involve oligomerization of SecYEG. Our results reveal that the organization of the lipid membrane plays a prominent role in the regulation of protein translocation and suggest that the regulation may be employed upon the bacterial adaptation to various habitat conditions.

Results

Unsaturated fatty acids stimulate protein translocation

The effect of the fatty acid structure on SecA : SecYEG-mediated translocation was examined using liposomes of defined and tailored lipid compositions. The inner membranes of *E. coli* are composed mainly of the zwitterionic lipid phosphatidylethanolamine (PE; up to 70 mol %) and anionic lipids, PG (20–25 mol%) and CL (3–5 mol %) [13]. Due to the small radius of their head groups, some PE species, such as DOPE, do not form planar lipid bilayers *in vitro*, and their gel-to-fluid transition temperatures are substantially higher than those of PG or another zwitterionic lipid phosphatidylcholine (PC) with the same fatty acid composition. Thus, to avoid potential nonlamellar structures and phase separation in the composite liposomes, PC lipids were employed here as the zwitterionic component. SecYEG was reconstituted into liposomes containing 30 mol % PG and 70 mol % PC; that way, the fraction of anionic lipids (PG) mirrored the abundance in the inner membrane of *E. coli* and should be sufficient to enable the electrostatically driven SecA : lipid interactions [3,5]. Indeed, the translocon remained active when reconstituted into POPC : POPG lipids, thus validating PC : PG liposomes as a functional membrane mimetic (Fig. 1B).

To examine the effect of the lipid-constituting UFAs on translocation, the fatty acid composition in the proteoliposomes was varied, while keeping the PC : PG molar ratio of 7 : 3 constant. Phospholipids composed

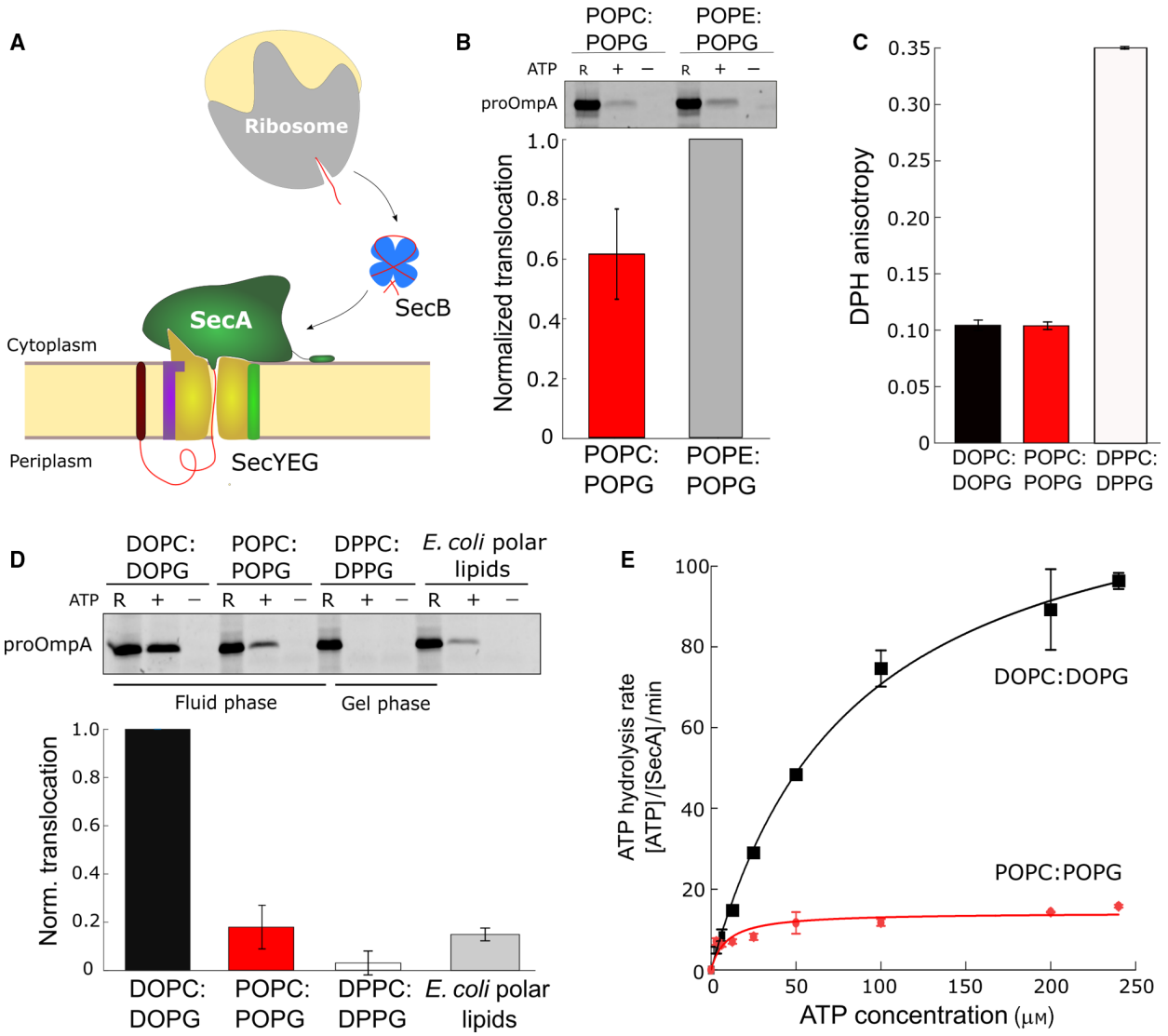

Fig. 1. Unsaturated fatty acids stimulate Sec-mediated translocation. (A) The primary bacterial pathway for protein translocation is composed of the cytoplasmic holdase chaperone SecB, the membrane-associated ATPase SecA and the transmembrane translocon SecYEG. (B) POPC : POPG lipid composition supports SecYEG activity. Translocation of the model substrate proOmpA was measured in SecYEG-containing proteoliposomes composed of 30 mol % POPG and 70 mol % zwitterionic lipids, either POPC or POPE. (C) Low fluorescence anisotropy of the DPH dye in either DOPC : DOPG or POPC : POPG confirms that both lipid bilayers are present in the fluid phase at 37 °C. In contrast, a high fluorescence anisotropy value measured in DPPC : DPPG membranes indicates the low-mobile gel phase. (D) Translocation of the preprotein proOmpA is sensitive to the content of the unsaturated fatty acids (UFAs), being maximal for DOPC : DOPG membranes. The translocation efficiency in DOPC : DOPG bilayers was used for normalization. Error bars show standard deviation (SD) values, as measured in triplicates. (E) The ATPase activity of SecA associated with proOmpA translocation is strongly stimulated in DOPC:DOPG proteoliposomes (K_M of 83 ± 6 μM). The uniform molar ratio of PC:PG lipids of 7 : 3 was used for all samples.

of dipalmitoyl (16 : 0/16 : 0, DP; no mono-UFA), 1-palmitoyl-2-oleoyl (16 : 0/18 : 1 Δ9-*cis*, PO; 50% mono-UFA) and dioleoyl (18 : 1/18 : 1 Δ9-*cis*, DO; 100% mono-UFA) fatty acids, as well as the natural extract of *E. coli* polar lipids (average mono-UFA content ~ 50 mol %), were tested. Fully saturated fatty acids of DPPC : DPPG lipids resulted in a gel-phase membrane (transition temperatures 42 °C), but both POPC : POPG and DOPC : DOPG membranes (phase transition temperatures −2 °C and −18 °C, respectively) were present in the disordered fluid phase, as confirmed by the fluorescence anisotropy analysis of

the conventional bilayer-incorporated reporter DPH (Fig. 1C) [14]. The membrane fluidity was essential for SecA : SecYEG-mediated translocation at 37 °C : Transport of the preprotein proOmpA was nearly zero in the gel-phase DPPC : DPPG liposomes; hence, the essential SecA : SecYEG dynamics must be severely suppressed (Fig. 1D). The fluid-phase membranes ensured the preprotein translocation, but the translocation efficiency manifested striking variations : DOPC : DOPG lipids strongly stimulated the activity of SecA : SecYEG, as up to 5-fold more proOmpA was accumulated in liposomes, in comparison to POPC : POPG membranes (Fig. 1D). The translocation efficiency correlated with the ATPase activity of SecA (Fig. 1E), suggesting that the length of the polypeptide chain translocated per cycle of ATP hydrolysis was not altered. The translocation in native *E. coli* extracts enriched with partially unsaturated PE lipids was substantially lower than in DOPC : DOPG liposomes, so that the stimulatory effect must originate from the fatty acid structure and presence of UFAs, but not the head group composition.

To investigate whether UFAs of phospholipids modulate the translocation rate, we analysed the kinetics of a single translocation cycle using the Förster's resonance energy transfer (FRET)-based transport assay [15]. The N-terminal proOmpA domain of the fusion preprotein proOmpA-DHFR is translocated into the liposome lumen (Fig. 2A). The preprotein stays trapped within the Sec complex, once the folded C-terminal DHFR domain blocks the SecA : SecYEG machinery, so the translocation cycle results in a stable stalled intermediate. Once the translocation intermediate is assembled, the fluorophores placed in the C-terminal part of proOmpA (Cyanine3, donor) and at the periplasmic side of SecYEG (Atto 643, acceptor) come into proximity allowing for FRET. The increase in the acceptor fluorescence is assigned to the assembly of the intermediate and, once recorded over time, it provides an insight into the translocation kinetics [15]. SecYEG reconstituted in the UFA-enriched DOPC : DOPG liposomes displayed approx. twofold higher rates of the intermediate formation compared to SecYEG in POPC : POPG liposomes (Fig. 2B and C). Next to that, the threefold lower amplitude of the FRET signal observed in POPC : POPG further suggested that a fraction of SecA : SecYEG complexes did not completely translocate the proOmpA domain, likely due to the slower translocation kinetics accompanied by inactivation of the temperature-labile SecA ATPase [16]. Together, the results of the functional assays reveal that UFAs within the physiologically fluid lipid membrane stimulate the efficiency of the SecA : SecYEG translocon and increase the rate of the polypeptide chain transport.

SecYEG stability and topology are not affected by fatty acid composition

The prominent effect of the lipid fatty acid composition on Sec-mediated translocation suggests that the hydrophobic core of the membrane could either affect stability and dynamics of the SecYEG translocon or be a novel factor that regulates SecA binding and SecA : SecYEG assembly. SecYEG is known to interact with specific lipids, such as PG and CL, and the interactions may cause heterogeneity in the structural dynamics [17–19]. To probe the effect of various environments on the translocon folding and stability, we established differential scanning fluorimetry (DSF) measurements, which report on the protein denaturation based on changes in the fluorescence emission of tryptophan residues [20]. Loss of the native protein structure leads to exposure of tryptophan residues to the aqueous solvent, so that their fluorescence is red-shifted. The SecYEG translocon contains eight tryptophan residues positioned at the ends of transmembrane helices (Fig. 3A), and their fluorescence was recorded over the temperature range from 20 to 90 °C. An abrupt change observed both in detergent micelles and in liposomes indicated the cooperative denaturation of the translocon (Fig. 3B). Notably, the lipid environment greatly stabilized SecYEG : The denaturation temperature T_m in DDM micelles was measured at 47 °C, but it increased to 66 °C in DOPC : DOPG liposomes (Fig. 3B). Variations in the lipid UFA content had a minor effect on the T_m value indicating that SecYEG was equally stable and correctly folded in the examined lipid bilayers (Fig. 3C). As the lipid composition had a minor effect on the reconstitution efficiency of the translocon, and POPC : POPG lipids rather favoured its functional topology in lipid membranes (Fig. 4A and B), UFA-specific SecYEG inactivation upon the reconstitution was excluded. Importantly, a recent mass spectrometry analysis of SecYEG-associated fatty acids in native membranes did not reveal deviations from the overall UFA distribution in *E. coli* inner membranes, so that the translocon does not form preferential interactions with specific fatty acids [17]. Finally, the $SecYEG^{prlA4}$ mutant, which demonstrates elevated preprotein translocation due to the altered structure of the central pore [21], was similarly sensitive to the UFA content as the wild-type translocon ($SecYEG^{WT}$, Fig. 4C). Thus, the dominant effect of UFAs on SecA : SecYEG-mediated translocation could not be related

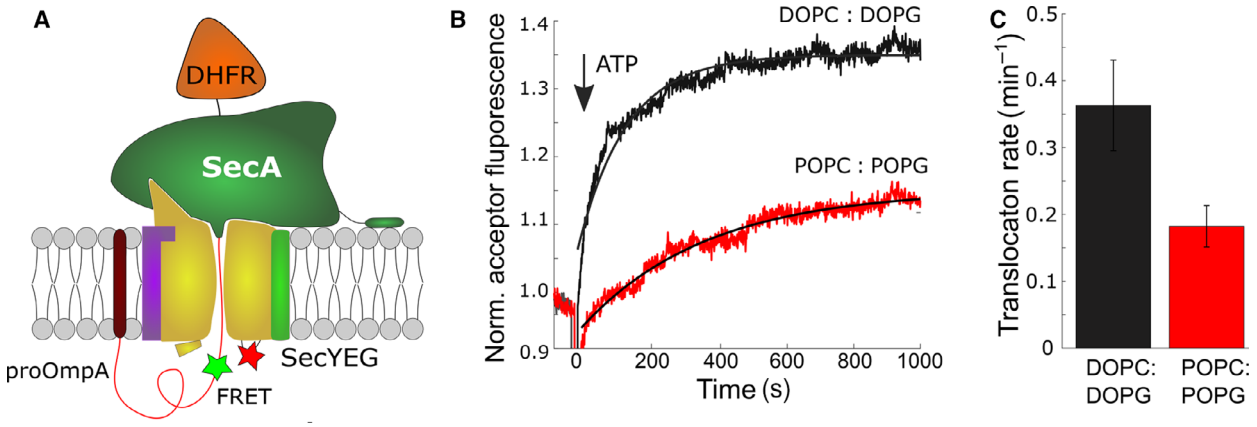

Fig. 2. Unsaturated fatty acids stimulate the kinetics of SecA : SecYEG translocation. (A) Scheme of the assembled translocation intermediate. The unfolded proOmpA domain is translocated via SecA : SecYEG, but the folded domain DHFR stalls the transport and jams the translocon. Two fluorophores positioned within proOmpA and at the periplasmic side of SecY allow for FRET once the stalled complex is formed. (B) Assembly of the translocation intermediate is followed as the fluorescence of the FRET acceptor is increasing with time after addition of ATP (arrow). The UFA-enriched DOPC : DOPG membranes (black) stimulate the proOmpA translocation and ensure formation of the stalled translocation intermediate. (C) Apparent translocation rates determined from the FRET-based assay validate the faster translocation reaction in the UFA-enriched DOPC : DOPG membrane. The molar ratio of PC : PG lipids of 7 : 3 was used for both samples. The error bars correspond to SD values based on measurements in duplicates.

to SecYEG : lipid contacts, but possibly originated from altered SecA : lipid interactions at the membrane interface.

Unsaturated fatty acids cause loose packing of lipid head groups

To study whether the lipid-constituting UFAs alter the lipid membrane organization, we employed the environment-sensitive dye laurdan to examine the lipid packing at the membrane : water interface. The dye spontaneously intercalates between the lipid head groups, and its general fluorescence polarization value decreases with higher water permeation, which is characteristic for loose lipid packing [22]. The fluorescence polarization measured in DOPC : DOPG liposomes was significantly lower than that in POPC : POPG membranes (-0.52 ± 0.02 vs. -0.40 ± 0.01; Fig. 5A), thus suggesting more disordered interface structure for the UFA-enriched lipid bilayer.

To scrutinize the lipid organization within the membrane at the molecular level, all-atom molecular dynamics (MD) simulations of DOPC : DOPG and POPC : POPG lipid bilayers were carried out. Both systems showed very similar electron density profiles and membrane thicknesses (Fig. 5B and Table 1). However, a comparison of the lateral pressure profiles and the lipid packing revealed prominent differences between these lipid bilayers (Fig. 5C–E). Pressure differences were observed in 1) the head group region (15–17 Å, the repulsive component is stronger in DOPC : DOPG); 2) close to the ester bonding (11–14 Å, attractive pressure in DOPC : DOPG); 3) in the region of the unsaturation (~ 5–10 Å, the repulsive component is stronger in DOPC : DOPG); and 4) in the membrane centre (0 Å, only the POPC : POPG system has a repulsive component). Thus, the presence of an additional double bond in DOPC : DOPG membrane shifts repulsive pressure from the acyl chain region towards the water interface, as suggested by analytical studies and found for similar lipid compositions of varying unsaturation degrees [23,24] and to some extent to the head group region. For DOPC : DOPG, the more attractive pressure at the ester bond region and at the membrane centre comes at the expense of the stronger repulsive components in the regions of the head groups and the unsaturation, reflecting more pronounced steric interactions between the polar groups and the acyl chains, respectively. Indeed, the packing density in the DOPC : DOPG system is higher in the ester bond region and the membrane centre, but lower in the regions of the head groups and the unsaturation (Fig. 5E), similar to what has been previously found for pure DOPC versus POPC systems [11]. The lower particle density on the surface of the membrane bilayer is associated with a larger area per lipid of the DOPC : DOPG system (70.25 ± 0.05 Å^2, mean ± SEM) compared to the POPC : POPG system (66.74 ± 0.02 Å^2; Fig. 5D and Table 1), in agreement with the results from laurdan

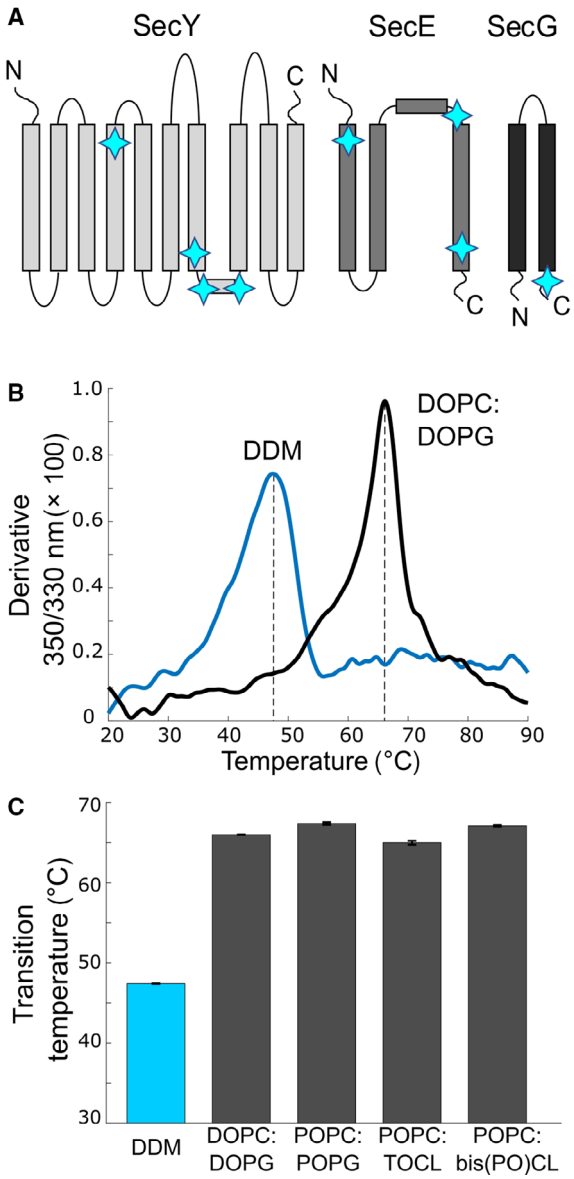

Fig. 3. The fatty acids content does not affect the stability and dynamics of the SecYEG translocon. (A) The scheme of the SecYEG secondary structure. Positions of the tryptophan residues are indicated with star symbols. Changes in tryptophan fluorescence were used to describe the thermal unfolding of SecYEG in DSF experiments. (B) Profiles of the thermal denaturation of SecYEG, as measured by differential scanning fluorometry based on the changes in the intrinsic tryptophan fluorescence. The lipid membrane substantially stabilizes the reconstituted translocon. (C) Thermal stability of SecYEG in liposomes is not influenced by the fatty acid composition of the membrane. Error bars show SD values, as measured in duplicates. The liposomes were composed of either 70 mol % PC and 30 mol % PG or 85 mol % PC and 15 mol % CL.

fluorescence (Fig. 5A). Thus, both experimental test and MD simulations indicate that the elevated UFA content leads to redistribution of the pressure within the membrane and induces looser packing of the lipid head groups.

Unsaturated fatty acids facilitate SecA binding to the lipid bilayer

SecA : lipid interactions at the membrane interface are recognized as an essential factor in Sec-mediated translocation [3,5,25]. Peripheral SecA : lipid binding may be a prerequisite to activate the ATPase and ensure the downstream SecA : SecYEG assembly [7,26]. Although the effect of UFAs on SecA binding has not yet been examined, it has been shown for several eukaryotic proteins that defects in the lipid packing and transiently exposed hydrophobic areas enhance the affinity of amphipathic helices to membranes [10,12]. The N-terminal tail of SecA (residues 1–25) forms an amphipathic helix that binds to and likely sinks into the lipid membrane in the presence of anionic head groups due to electrostatic interactions (Fig. 6A and B) [27]. In unbiased MD simulations, taking the surface area occupied by the lipids into consideration, the SecA N-terminal tail preferentially interacts with DOPG and POPG lipid head groups mainly through its basic residues (Figs. 6C and D), with a higher contribution from residues 13 to 20 within the C-terminal half of the polypeptide. Deletion of the N-terminal tail abolishes the protein translocation [28]. Since the activity can be restored *in vitro* once the tagged SecA is artificially anchored to proteoliposomes, the primary role of the N terminus is to facilitate SecA binding to the membrane.

To test whether the UFA content and the altered lipid packing affect the SecA : membrane interaction, binding of SecA to liposomes was examined. Once bound to the lipid leaflet, SecA can float with liposomes through a sucrose density gradient, thus allowing to estimate the binding efficiency (Fig. 7A). SecA readily interacted with PG-containing liposomes, while the binding was nearly abolished for SecA mutant lacking the N-terminal 20 amino acids (Fig. 7B). In agreement with earlier results, the mutant could not support preprotein translocation. Increasing the salt concentration from 50 to 500 mM reduced SecA binding to POPC : POPG liposomes by ~ 80% (Fig. 7C), so SecA : lipid binding was salt-sensitive, as expected for the electrostatics-driven interaction. Notably, for DOPC : DOPG liposomes, the reduction was limited

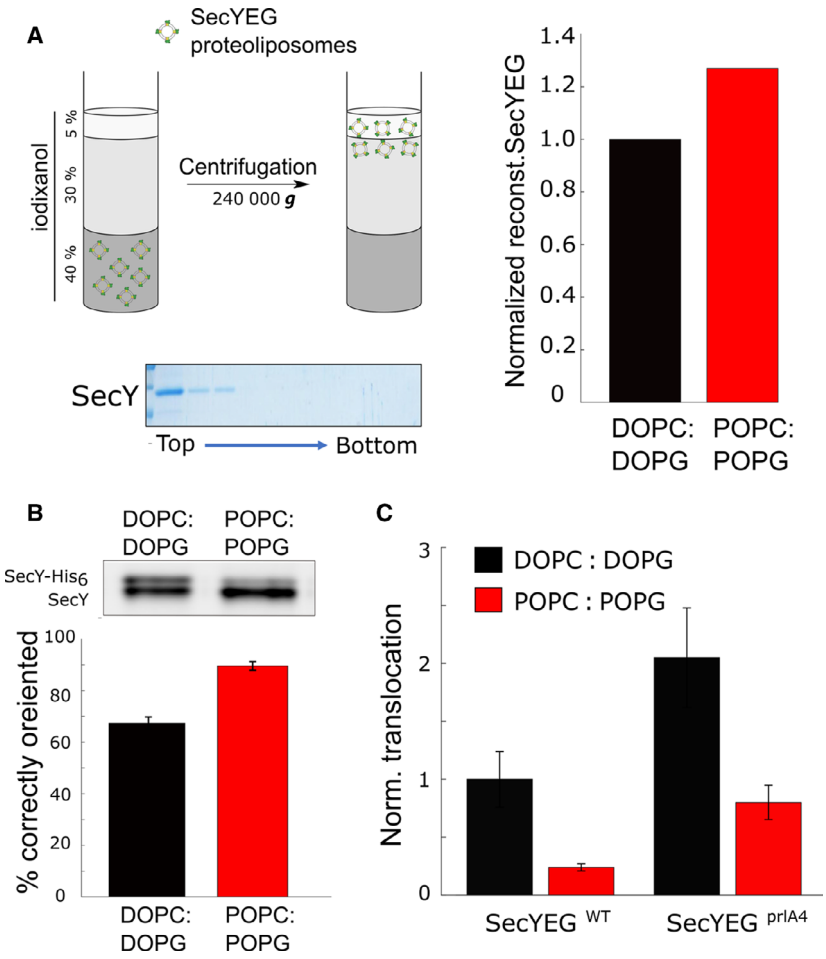

Fig. 4. (A) Flotation assay in iodixanol density gradient using SecYEG proteoliposomes demonstrated nearly equal reconstitution efficiency of the translocon for DOPC : DOPG or POPC : POPG lipids. The example SDS/PAGE shows the distribution of SecY reconstituted into DOPC : DOPG liposomes. (B) Site-specific cleavage of the N-terminal poly-histidine tag of SecY subunit by enterokinase reports on the accessibility of the tag in liposomes, and so reveals the orientation of reconstituted SecYEG. In POPC : POPG liposomes nearly 80% of the translocons were exposed to the protease, and so acquired the functionally relevant orientation. (C) The activity of the up-regulated translocon mutant SecYEG^{prlA4} is equally sensitive to the UFA content as the wild-type translocon (SecYEG^{WT}), suggesting that UFAs play a SecYEG-independent role in the translocation. Error bars show SD values, as measured in duplicates. The uniform molar ratio of PC : PG lipids of 7 : 3 was used for all samples.

to 40% only, and the amount of SecA bound to DOPC : DOPG liposomes exceeded that bound to POPC : POPG over the whole range of tested salt concentrations. The difference reached fivefold at 500 mM KCl, thus confirming the effect of the lipid packing on SecA : membrane interaction and highlighting the role of hydrophobic interactions at the loosely packed interface.

Notably, when POPC was substituted with DOPC in a stepwise manner, both SecA binding and the preprotein translocation in SecYEG proteoliposomes continuously increased, and introducing DOPG instead of POPG had a similar effect (Figs 8A and B). This clear correlation supported the hypothesis that the UFA-enhanced SecA : lipid interactions promote SecA : SecYEG translocation. We questioned then whether the configuration of the double bond within the UFA affects SecA : membrane interactions. Introducing a *trans*-bond in position Δ9 in both fatty acids of PC had a pronounced effect on the membrane properties : although the lipid bilayer resided in the fluid phase (phase transition temperature ~ 12 °C), the laurdan fluorescence indicated tight packing within the head group region similar to UFA-poor POPC : POPG membranes (Fig. 5A). The increase in the lipid packing led to suppressed binding of SecA and finally caused approx. 7-fold reduction in SecA : SecYEG-mediated translocation (Figs 8C and D). Alike, binding of SecA to gel-phase membranes DPPC : DPPG was suppressed three- to fourfold even at the low salt concentration (50 mM KCl; Fig. 8C), despite the presence of the anionic lipids, and correlated with the loss of SecA : SecYEG activity (Fig. 1C).

Aiming for quantitative characterization of SecA : lipid interactions, surface Plasmon resonance (SPR) experiments were carried out. The steady-state response upon binding of SecA to the chip-anchored liposomes was strongly enhanced in UFA-based DOPC : DOPG membranes (Fig. 9A). The measurements over a range of SecA concentrations provided an estimate of the apparent dissociation constant K_D for SecA : lipid interactions (Fig. 9B). In the presence

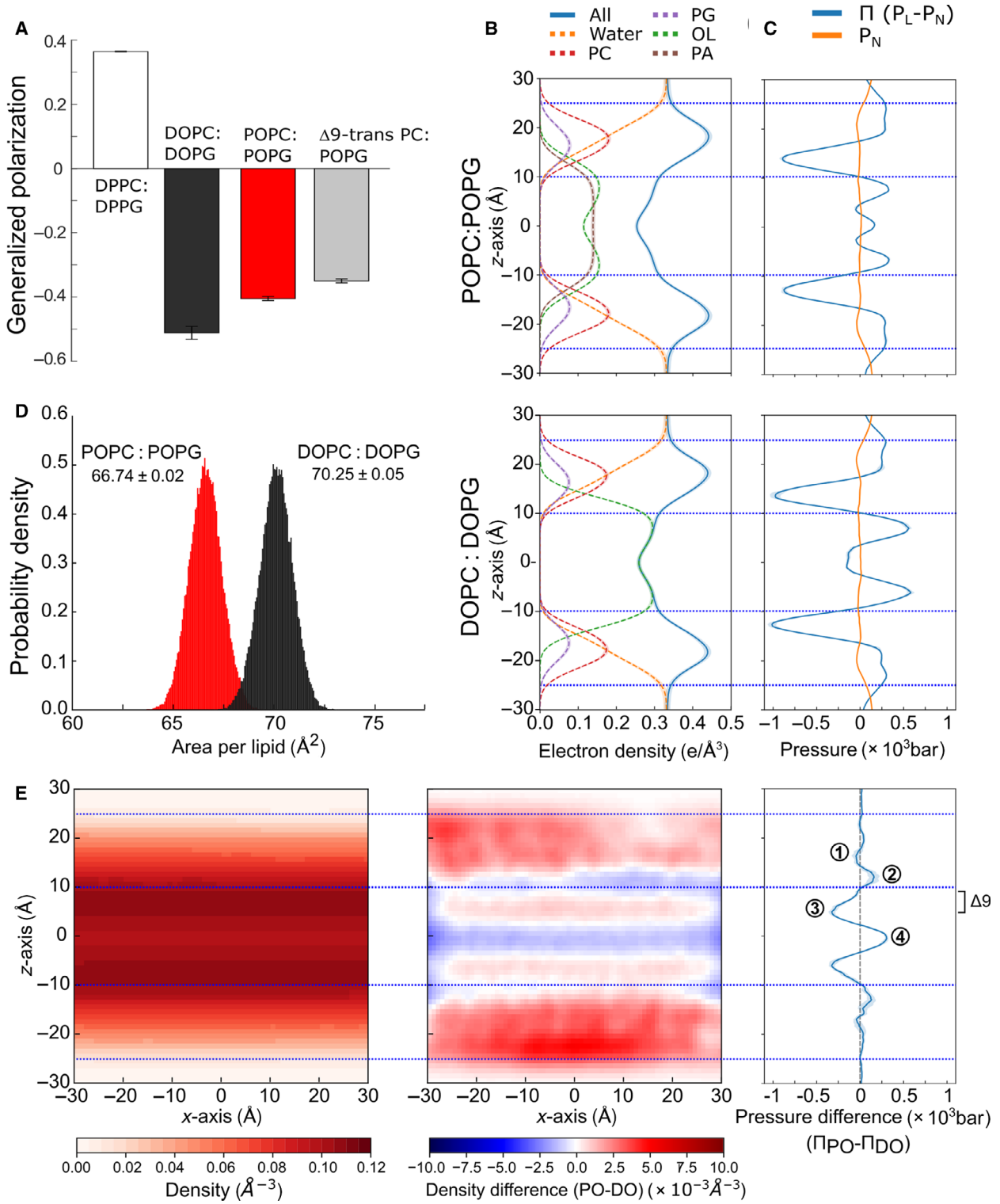

of 150 mM KCl and 5 mM $MgCl_2$, SecA showed a 1.7-fold higher affinity to DOPC : DOPG membranes (125 ± 5 nM) than to POPC : POPG membranes (210 ± 45 nM). In agreement with the flotation assay (Fig. 7C), SecA : lipid binding was suppressed at elevated salt concentration of 300 mM KCl for both

Fig. 5. Fatty acid structure determines the biophysical properties of lipid bilayers. (A) General polarization of the laurdan dye suggests a looser packing of the lipid head groups in *cis*-UFA-enriched lipid bilayers (DOPC : DOPG). Error bars show SD values, as measured in triplicates. (B) Electron density profiles of POPC : POPG (top) and DOPC : DOPG (bottom) bilayers. The profiles provide information regarding the location of the membrane components along the plane normal. PC: phosphatidylcholine headgroup; PG: phosphatidylglycerol headgroup; OL: oleate acyl chain; PA: palmitate acyl chain. (C) Lateral pressure profile (Π) of the simulated bilayers, showing the characteristic negative component associated with the membrane : solvent interface (see the water density drop in B) and a central positive pressure component in the POPC : POPG system (top) that is absent in the DOPC : DOPG bilayer [24]. P_L and P_N are lateral and normal components of the pressure tensor. (D) Distributions of the area per lipid in the simulated bilayers. The area per lipid is significantly higher ($P < 0.001$; Tukey HSD test, Table 1) in the bilayer composed of DOPC : DOPG, despite overall similar electron density profiles. (E) 2D number density of lipids on the x z plane of the POPC : POPG bilayer and the difference of the x z densities and lateral pressure profiles of (POPC : POPG–DOPC : DOPG). In the DOPC : DOPG bilayer, the density is higher in the membrane centre and in the region of the ester bonds, but lower in the region of the fatty acid unsaturation and the polar head groups. In the pressure profile, two UFAs cause a higher repulsive component in the head group region (1), a more attractive pressure close to the ester bonds (2), a higher repulsive component in the region corresponding to the double bonds (3), and a lower repulsion in the centre of the membrane bilayer (4). The regions with a more attractive component in the DOPC : DOPG system (2,4) relate to a relatively higher density of lipids. 'Δ9' indicates the region where the unsaturated bonds in the upper leaflet of the lipid bilayer are located (see B, green curves). All values from B to E were calculated from all-atom MD simulations based on five independent replicas. The uniform molar ratio of PC : PG lipids of 7 : 3 was used for all experiments.

DOPC : DOPG and POPC:POPG, where the apparent K_D decreased to $\simeq 1.2$ μM and 2.4 μM, respectively (Fig. 9B). Notably, while the determined change in the affinity was small, the SPR response signal was nearly twofold higher upon SecA binding to DOPC : DOPG liposomes, even at the saturation level (1050 vs. 600 response units, Fig. 9A). As the amounts of immobilized unilamellar liposomes did not vary between samples, the differences in the SPR response signal cannot be related to the available SecA binding sites at the liposome surface. Instead, it seems feasible that the DOPC : DOPG membranes promote binding of SecA dimers, previously described in the cellular membranes [29,30].

To exclude that binding was affected by the non-physiological positive curvature of the liposomes, a complementary experiment was carried out using planar supported lipid bilayers (SLBs) deposited on a quartz crystal microbalance (QCM) chip [31]. Liposomes were noncovalently adsorbed on the quartz chip surface and fused to form continuous SLBs (Fig. 10A and B). Subsequent SecA binding increased the mass adsorbed on the quartz chip, which affected its resonance frequency (Fig. 10C and D). Depending on SecA concentration, the ATPase binding to DOPC : DOPG membranes measured in 150 mM KCl and 5 mM $MgCl_2$ was 25 to 50% higher than to POPC : POPG membranes, pointing to the higher mass of the protein accumulated at the membrane interface, also upon reaching the saturation of binding (Fig. 10D and E). The apparent K_D values were 91 nM and 161 nM, respectively (Fig. 10F), in good agreement with the SPR data. Thus, biochemical and biophysical assays confirmed the differential binding of SecA to lipid bilayers depending on the UFA content and the associated lipid head group packing, and the binding efficiency correlated with the translocation activity of the SecA : SecYEG complex.

Tetraoleoyl-cardiolipin stimulates SecA binding and preprotein transport

The inner membranes of *E. coli* and other Gram-negative bacteria commonly contain a minor fraction of cardiolipin (CL) molecules [13], and a recent mass spectrometry analysis revealed that the most abundant

Table 1. Area per lipid and membrane thickness measured in MD simulations of the investigated systems.[a]

Head group	POPC : POPG70 : 30	DOPC : DOPG 70 : 30	POPC : bis(PO)CL 85 : 15	POPC : TOCL 85 : 15
PC APL[b,*]	67.14 (0.05)	70.68 (0.07)	73.05 (0.12)	74.13 (0.12)
PG APL[b,*]	65.86 (0.19)	69.28 (0.18)	-	-
CL APL[b,*]	-	-	79.23 (0.65)	80.38 (0.23)
Average APL[c,*]	66.74 (0.02)	70.25 (0.05)	73.97 (0.09)	75.06 (0.07)
Thickness[d]	37.38 (0.01)	37.06 (0.02)	38.71 (0.04)	38.64 (0.04)

[a]All measurements were done over the last 800 ns of five 1 μs replicas and are shown as the mean of replica means (standard error of the mean); [b]Area per lipid (Å^2) as measured by APL@Voro [70]; [c]Area per lipid (Å^2) measured as the xy-sectional area of the average simulation box used per lipid; [d]Membrane thickness (Å) measured as the distance between the z-coordinates of the centres of mass of the phosphorous atoms of each leaflet; [*]The pairwise difference of the mean across all systems is statistically significant ($P < 0.001$, Tukey HSD).

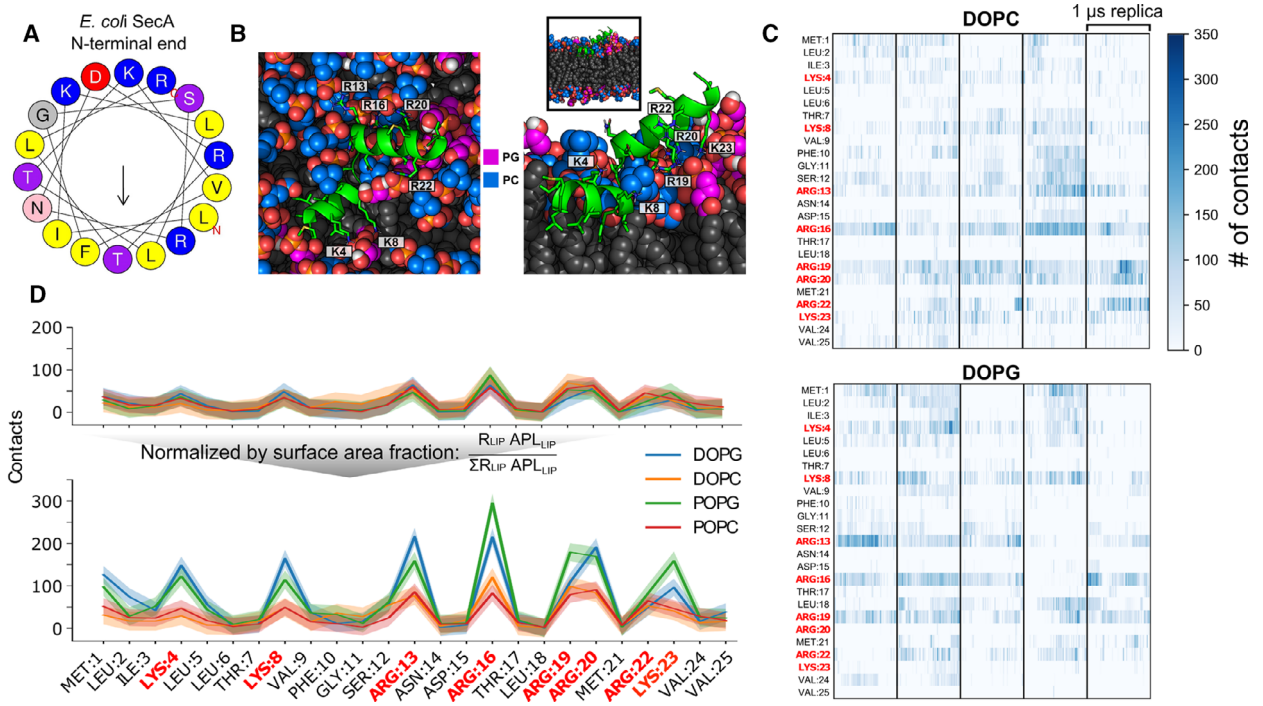

Fig. 6. SecA : membrane association is mediated by unsaturated fatty acids. (A) Helix wheel projection of the N-terminal end of *E. coli* SecA of the putative amphipathic helix (via heliquest.ipmc.cnrs.fr). The hydrophobic moment (~ 0.4) is indicated with the arrow. (B) A binding pose of the N-terminal amphipathic helix of SecA at the interface of the lipid bilayer after 1 μs of MD simulation (DOPC : DOPG, replica 4). Basic residues that show pronounced interactions with the head groups are highlighted. (C) Interactions of the SecA N-terminal helix (residues 1 to 25) with DOPC : DOPG lipids over MD simulations of 1 μs length. Per-residue contacts with membrane headgroups in each replica are shown. Cationic residues are highlighted in red. (D) Mean per-residue contacts of the N-terminal SecA peptide with head groups in DOPC : DOPG and POPC : POPG membranes over MD simulations of 1 μs length, with the coloured background showing the standard error of the mean over 5 replicas, as exemplary shown in C. When the absolute contacts are measured (top), comparable results are obtained irrespective of the head group considered. If the surface area occupied by the lipid types is taken into account (bottom, where R_{LIP} represents the ratio factor and APL_{LIP} the area per lipid for each lipid type reported in Table 1), negatively charged PG lipids show a higher propensity to interact with positively charged residues than the neutral PC head groups. The uniform molar ratio of PC : PG lipids of 7 : 3 was used for all simulations.

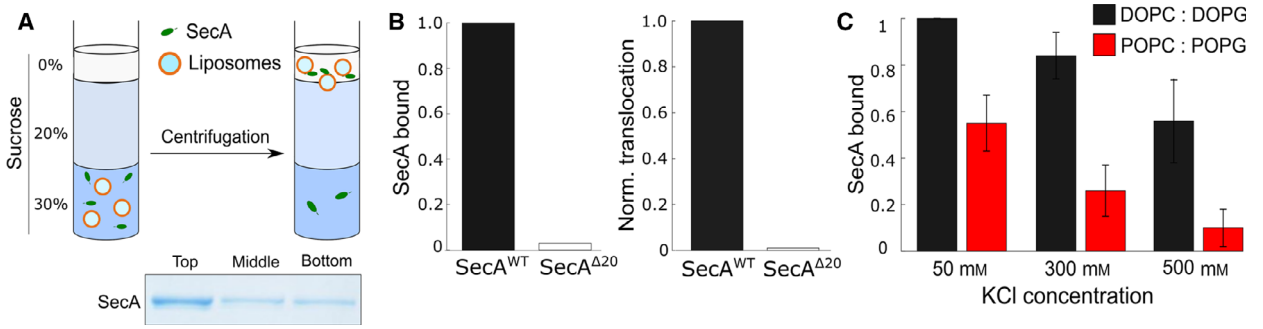

Fig. 7. SecA : membrane association is mediated by unsaturated fatty acids (A) Scheme of the flotation assay to probe SecA : lipid interactions. Upon the centrifugation, the liposomes loaded with aqueous buffer migrate to the top of the sucrose density gradient. Liposome-bound SecA is found in the top layer of the gradient, while free SecA remains in the bottom fraction. (B) Deletion of SecA N-terminal helix abolishes lipid binding as tested via the flotation assay and eliminates SecA : SecYEG translocation activity in DOPC : DOPG liposomes. (C) The flotation assay reveals UFA-dependent and salt-sensitive binding of SecA to the liposomes. Error bars show SD values, as measured in triplicates. The uniform molar ratio of PC : PG lipids of 7 : 3 was used for preparing the liposomes.

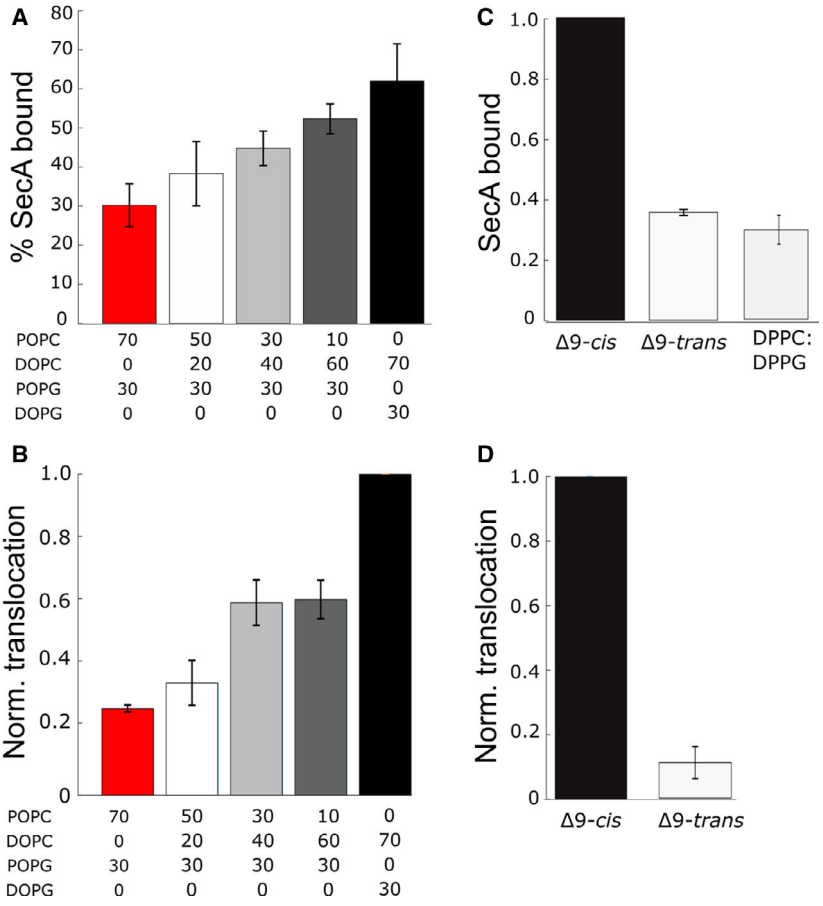

Fig. 8. UFA-dependent SecA : lipid binding correlates with the SecA : SecYEG activity. (A) Upon the gradual increase of the UFA content, the SecA : lipid binding (flotation assay) correlates with the translocation activity of SecA : SecYEG complex (B). (C) SecA binding is hindered in the presence of Δ9-*trans* UFA, that leads to the inhibition of the preprotein translocation by SecA : SecYEG (D). Thus, the configuration of the unsaturated fatty acid determines the functionality of SecA : SecYEG complex. All liposomes contained 30 mol % DOPG and 70 mol % indicated 18 : 1 PC lipids. Alike, SecA binding to gel-phase liposomes composed of DPPC : DPPG lipids is strongly suppressed in comparison to fluid-phase liposomes (DOPC : DOPG). Error bars show SD values, as measured either in triplicates (SecA binding) or duplicates (translocation).

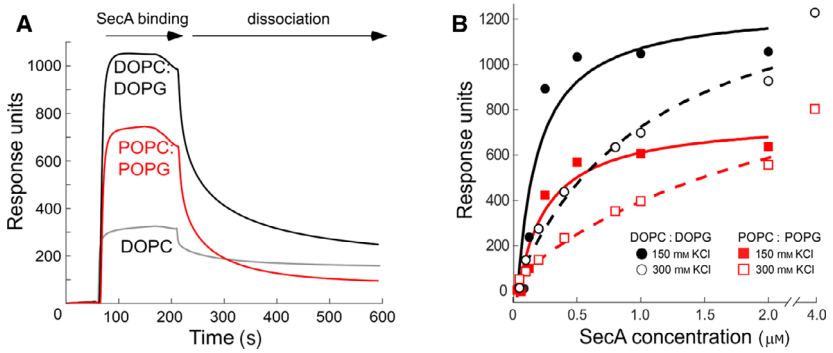

Fig. 9. Unsaturated fatty acids enhance the affinity of SecA : liposome interactions. (A) Surface Plasmon resonance (SPR) sensograms of SecA (concentration 500 nM) binding to immobilized liposomes, followed by the dissociation phase. Charge-neutral membranes composed of pure DOPC were used as a negative control. (B) Analysis of the steady-state SPR response over a range of SecA concentrations (31 nM to 2 μM) reveals enhanced binding to DOPC : DOPG membranes. SecA : lipid interactions are sensitive to the ionic strength, being weakened at the elevated salt concentration. The uniform molar ratio of PC : PG lipids of 7 : 3 was used for preparing the liposomes.

CL species in the *E. coli* membrane contain four mono-UFAs [17]. CL molecules are enriched two- to threefold in the proximity of the translocon [17,18], and it has been suggested that CL facilitates SecYEG homo-dimerization, but may also serve as an acceptor for protons to contribute to the proton motive force [18]. However, the functional translocon *in vitro* and *in vivo* is built of monomeric SecYEG, and no stimulatory effect of CL on SecA : SecYEG activity in the UFA-enriched membranes was observed [15,32]. Thus,

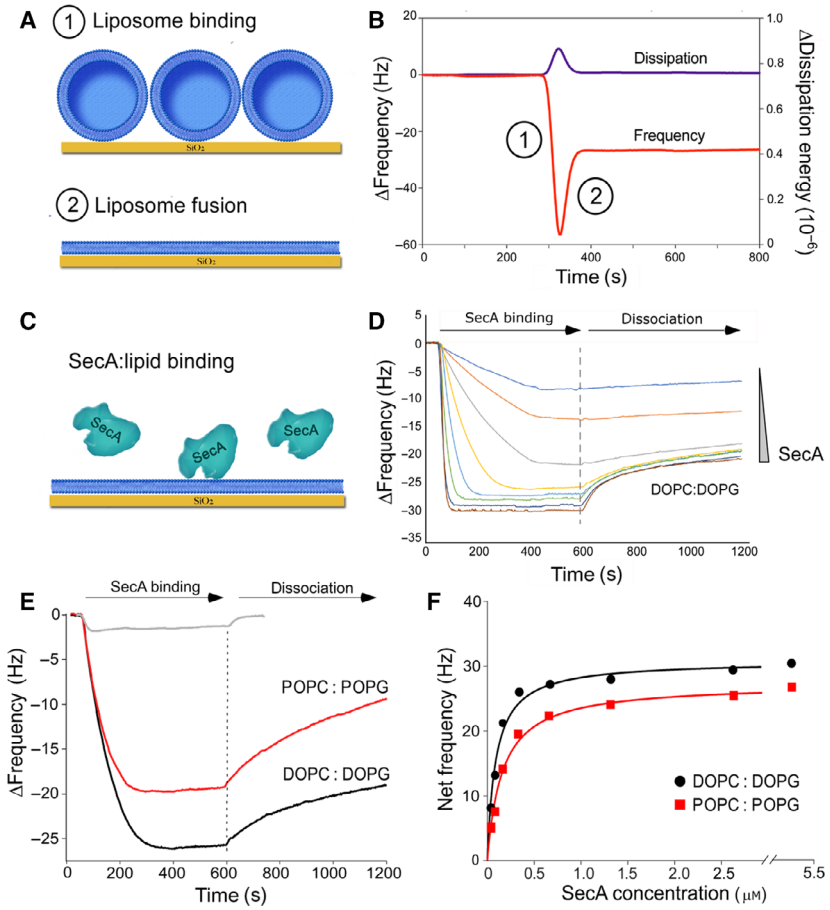

Fig. 10. Unsaturated fatty acids enhance SecA binding to the planar lipid bilayers (A) Formation of the lipid bilayer on the quartz crystal microbalance (QCM) chip surface. Liposomes are bound to the surface at high density, and their fusion in the presence of calcium leads to the formation of the supported lipid bilayer. (B) The attachment and the fusion of liposomes are observed as changes in the oscillation frequency of the chip (stages 1 and 2). An increase in the energy dissipation upon the liposome attachment is due to the large volume of encapsulated water, which is further released upon fusion (stage 2). (C, D) Measuring SecA binding to the lipid bilayer via changes in the oscillation frequency. SecA was injected in the buffer flow over DOPC : DOPG bilayer to monitor the association and dissociation stages. SecA concentration ranged from 40 nM to 5.25 μM (twofold dilution per titration step). (E) QCM sensograms of 800 nM SecA binding to planar lipid bilayers, followed by the dissociation phase. Charge-neutral membranes composed of pure DOPC were used as a negative control. (F) Analysis of the steady-state frequency change over a range of SecA concentrations (40 nM to 5.25 μM) reveals enhanced binding of SecA to DOPC : DOPG membranes. The uniform molar ratio of PC : PG lipids of 7 : 3 was used for all samples.

the role of CL in SecA : SecYEG activity has remained intensively disputed [7,33].

In light of the discovered effect of UFAs on Sec-mediated translocation, we questioned whether UFA-enriched CL, such as tetraoleoyl-CL (TOCL), may recruit SecA to the lipid membrane and to enhance the preprotein transport. To test this hypothesis, SecYEG was reconstituted in POPC : POPG : TOCL membranes with a variable amount of TOCL. To keep the net negative charge at the membrane interface constant, the variations in the CL content were compensated by tuning the POPG fraction. Changing the CL fraction from 0 to 15 mol % increased the translocation activity up to 10-fold, indicating that TOCL is indeed a potent stimulator of protein translocation (Fig. 11A). To exclude potential dimerization of SecYEG in the presence of CL, the translocons were reconstituted into nanodiscs as monomers, and the translocation efficiency in the presence of TOCL was determined using the FRET-based assay [34,35]. The dimensions of nanodiscs (outer diameter ~ 15 nm) and the lipid : protein ratio used upon the reconstitution ensured that ~ 200 lipid molecules were embedded in each nanodisc [36]. TOCL strongly stimulated the translocation efficiency and kinetics, despite the nanodisc boundaries physically prevented dimerization of

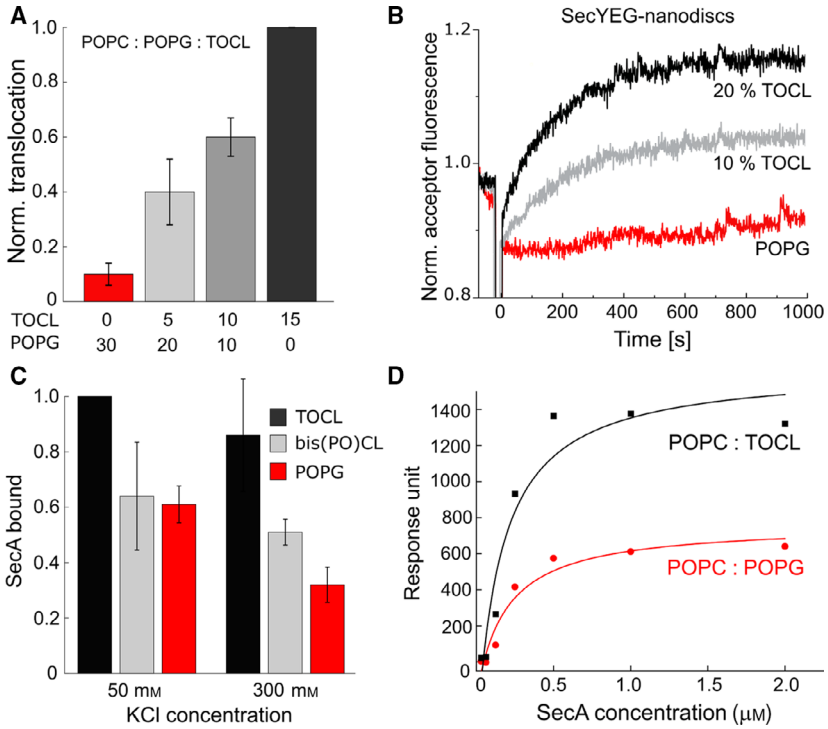

Fig. 11. UFA-enriched cardiolipin stimulates Sec-mediated translocation. (A) Elevated concentrations of tetraoleoyl-cardiolipin (TOCL) stimulate preprotein transport into liposomes. SecYEG-containing liposomes consisted of POPC and POPG/TOCL mixture at the indicated molar ratios to maintain the uniform electrostatic interactions at the interface. The error bars correspond to SD values based on measurements in duplicates. (B) FRET-based translocation assay shows increased activity of monomeric SecYEG in nanodiscs in presence of TOCL. The stimulated activity is achieved without oligomerization of the translocon. POPG : TOCL ratios were identical to those in panel (A). (C) Flotation assay confirms the preferential interactions of SecA with UFA-enriched TOCL. Binding to TOCL-containing membranes is the least affected by the elevated ionic strength, so the interactions with UFAs promote the membrane-bound form of SecA. Lipid membranes were composed of either 70 mol % POPC and 30 mol % POPG or 85 mol % POPC and 15 mol % CL. The error bars correspond to SD values based on measurements in duplicates. (D) SPR experiments show enhanced binding of SecA to liposomes containing POPC and 15 mol % TOCL in comparison to liposomes with POPC and 30 mol % POPG, despite the identical charge density at the interface.

SecYEG (Fig. 11B). While TOCL did not affect the stability of SecYEG (T_m ~ 66 °C, Fig. 3C), binding of SecA to TOCL-containing liposomes was enhanced compared to POPC : POPG, as tested by flotation assay and SPR (Fig. 11C and D). Although additional effects of interactions of TOCL with the active SecA : SecYEG complex are possible, our data demonstrate that even in the absence of the proton motive force, TOCL favours SecA : lipid interactions at the membrane interface and stimulates the translocation.

Effect of cardiolipin on translocation depends on the fatty acid structure

Does the CL-mediated stimulation originate from the UFA content, or may it be determined by the high charge density within the CL head group? To address this question, two CL variants, TOCL (four UFAs) and bis(palmitoyloleoyl)-CL (bis(PO)CL, two UFAs), were examined with MD simulations and in model liposomes. Exchanging POPG with either TOCL or bis(PO)CL in the simulated bilayer (POPC : CL molar ratio 85 : 15) caused significant increases in the overall and lipid type-specific area per lipid with respect to the POPC : POPG system, and the change was the most pronounced for the POPC : TOCL bilayer (Table 1). Given the larger size of cardiolipins, an increase in the average area per lipid was to be expected, but, notably, the effect also comprised the other lipid types in the bilayer. As such, the area per POPC molecule increased by 10%, from 67 Å^2 (POPC : POPG bilayer) to 74 Å^2 (POPC : TOCL bilayer). The pressure profiles (Fig. 12A) and the particle density difference of the simulated bilayers with TOCL or bis(PO)CL indicate that TOCL causes a shift of the repulsive pressure from the acyl chain region towards the water interface, with a higher particle density in the ester bond region and lower density in the head group region (Fig. 12B),

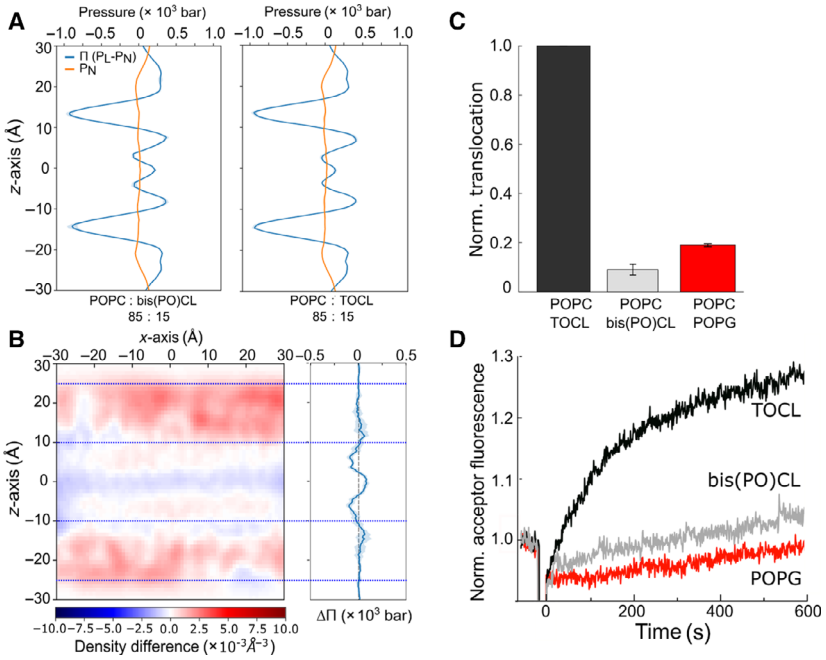

Fig. 12. UFA-enriched cardiolipin stimulates Sec-mediated translocation. (A, B) The difference in 2D density profile and lateral pressure obtained by MD simulations for POPC : CL lipid bilayers (bis(PO)CL-TOCL) reveal a qualitatively similar trend as that observed for the POPC : POPG – DOPC : DOPG case (Figure 5). (C, D) The translocation efficiency and the translocation rate probed in the FRET-based assay using liposome-reconstituted SecYEG demonstrate the stimulatory effect of TOCL that agrees with the enhanced SecA binding (Figure 11C). Lipid membranes were composed of either 70 mol % POPC and 30 mol % POPG or 85 mol % POPC and 15 mol % CL. The error bars correspond to SD values based on measurements in duplicates.

in a qualitative agreement with the results acquired from the simulated DOPC : DOPG and POPC : POPG bilayers (Fig. 3). Thus, both CL types caused substantial restructuring of the lipid bilayer compared to the POPC : POPG system, as indicated by the change in the lipid packing and the transmembrane distribution of the pressure density.

Notably, the density difference calculated between the bilayers with TOCL and bis(PO)CL is smaller in magnitude than the value determined for pure DOPC : DOPG and POPC : POPG membranes. In agreement with the computed predictions, the laurdan fluorescence in CL-containing liposomes manifested a modest, although significant, change in the polarization value upon variations in the UFA content : the general polarization increased from -0.389 ± 0.005 (15 mol % TOCL) to -0.335 ± 0.012 (15 mol % bis(PO)CL). To probe the effect of different CLs on SecA : SecYEG activity, functional tests were carried out using POPC : CL liposomes. SecA : lipid interactions were enhanced by TOCL, but not bis(PO)CL species in comparison to pure POPC : POPG membranes, suggesting that the UFA abundance, but not the charge density within the CL, affect the ATPase binding (Fig. 11C). Furthermore, the UFA-dependent binding of SecA converted into the differential effect of CLs on preprotein transport : while no stimulation was provided by bis(PO)CL, 15 mol % TOCL stimulated the activity of SecA : SecYEG (Fig. 12C). The FRET-based translocation assay in SecYEG-containing proteoliposomes further confirmed a prominent effect of TOCL, but not bis(PO)CL on the translocon activity (Fig. 12D), so the composition of the membrane core influenced the transport rate of a polypeptide chain.

Discussion

The diversity of lipids found in prokaryotic and eukaryotic cellular membranes greatly determines physicochemical properties of the bulk membrane, but also promotes formation of functional membrane domains and mediates specific interactions with the membrane-associated proteins [37,38]. Both bulk and specific local properties of the lipid bilayer may regulate the functionality of membrane-embedded complexes, being crucial for cellular pathways, such as energy metabolism, signal transduction and the broad repertoire of transport processes. Protein translocation via the essential Sec machinery is a well-known example, where the naturally abundant anionic lipids are required for the assembly of the functional SecA : SecYEG complex [3,7,26]. While the contribution of electrostatic interactions at the interface has been extensively examined, here we reveal that the protein translocation is sensitive to changes in the fatty acid composition of the phospholipids. The protein translocation is augmented fivefold upon increasing the content of dioleoyl fatty acids in the range from 50 to 100 mol %, although the fluidity of the bilayer is not changed. While neither stability nor topology of the translocon SecYEG is affected by the lipid composition, the elevated translocation correlates with the

increased binding of the ATPase SecA to the UFA-enriched lipid bilayer. The stimulatory effect of UFAs on SecA binding is well-pronounced at the elevated salt concentrations, pointing to the previously not appreciated role of hydrophobic interactions.

While it was generally believed that SecA is equally distributed between the inner membrane interface and the cytoplasm, as determined by subcellular fractionation studies [27,29], the most recent results based on SecA imaging *in vivo* revealed that approx. 90% of the ATPase pool is found at the membrane, either interacting with the translocon or being bound to the lipid leaflet [30]. SecA localization at the cellular membrane appears to be sensitive to physiological factors, such as proton motive force and mechanical stress induced upon the cell lysis [30], and the recruitment of SecA to the membrane is essential for the translocation [26,28,39]. SecA : lipid binding is largely mediated by the N-terminal amphipathic helix of the ATPase : The helix is essential for interactions with the membrane, where it extensively binds anionic lipids via lysine and arginine residues at the polar side [28,40,41]. Further partitioning of the helix into the lipid leaflet, however, must rely on interactions with the hydrophobic fatty acids. Our all-atom MD simulations together with biophysical analysis of the lipid bilayer structure suggest that UFAs induce irregularities and looser head group packing at the membrane : solvent interface. A similar effect must have been observed in the early study on SecA : SecYEG, when DOPE was described as a potent stimulator of the translocon machinery [5]. The small PE head group combined with two UFA chains results in extensive packing defects at the membrane interface [10]. In the simplest scenario, those interfacial features allow the amphipathic helix of SecA to access the transiently exposed hydrophobic regions and facilitate partitioning of the helix into the bilayer [10,25,41]. At the elevated salt concentrations, the electrostatic coupling of the protein to the anionic lipids largely deteriorates, and the membrane-bound state of SecA depends on nonpolar contacts with the membrane interior. In combination with the previous studies, our data suggest that the hydrophobic interactions enhance the propensity of SecA to bind to the lipid membrane over a broad range of conditions, and the affinity is jointly determined by the electrostatic and apolar interactions at the interface.

Once bound to the lipid interface, SecA undergoes two-dimensional diffusion within the lipid leaflet prior docking on the SecYEG translocon [26,30]. Thus, the elevated concentration of the membrane-bound SecA favours the downstream assembly of the SecA : SecYEG complex and stimulates the preprotein transport, as observed in our experiments. Notably, the quantitative analysis of SecA : lipid interactions via SPR and QCM reveals a modest 2- to 3-fold increase in the affinity, while the translocation activity increased up to ten-fold (POPC : POPG vs. POPC : TOCL). This may indicate that the preprotein translocation involves multiple SecA molecules, which diffuse at the membrane interface and transiently bind the translocon, as either dimers or monomers, to perform cycles of translocation. Despite the extensive research, neither the quaternary state and dynamics of SecA nor its processivity in translocation have been clarified [42–44]. Recent reports have suggested that the oligomeric state of the membrane-bound SecA depends on the membrane lipid composition, with monomers being prevalent for PO-type lipids [40,45], although the dimeric form of SecA has been described at the intact cellular membrane [27,30]. Notably, both SPR and QCM experiments showed changes in the net signal, that is Plasmon resonance response and the quartz resonance frequency upon binding saturation. The difference between SecA binding to POPC : POPG or DOPC : DOPG reached nearly 100%, as measured by SPR. The observed response levels likely reflect different amounts of SecA bound at the examined lipid interfaces, as could be related to different oligomeric states of the ATPase, that is dimers at DOPC : DOPG and monomers at POPC : POPG bilayers. Thus, it deserves further evaluation whether the membrane structure, including the UFA-mediated lipid packing, influences SecA quaternary dynamics.

The requirement of CL for SecA : SecYEG-mediated translocation has been intensively debated, and specific SecYEG : CL and SecA : CL contacts and CL-induced protein dimerization, which promote the preprotein transport, have been proposed [33,46,47]. Lately, the stimulatory effect of CL has been described in the presence of the proton motive force [18]. Here, we demonstrate that the UFA-enriched TOCL, but not bis(PO)CL, contributes to SecA binding and enhances the translocation up to 10-fold. Furthermore, the translocation experiments in nanodiscs allowed to rule out the translocon dimerization upon the translocation. Thus, UFA-mediated SecA binding does not depend on lipid species, but strongly correlates with the bulkhead group packing at the membrane interface. Interestingly though, MD simulations and measurements of the laurdan fluorescence reveal relatively small differences between lipid membranes containing TOCL or bis(PO)CL, while only TOCL is potent to stimulate the translocation. It suggests that more intricate mechanisms should be considered to interpret the effect of UFAs on SecA binding and translocation, for example formation of CL-specific domains within the otherwise miscible lipid membrane [48], restructuring

of the annular lipids upon SecA binding, or UFA-dependent dynamics of the SecA : SecYEG complex.

The experiments presented here are based on a reconstituted system that contains the core components of the Sec translocation pathway, that is SecB as a targeting factor, SecA motor protein and membrane-embedded translocation channel SecYEG, while a number of physiological factors, such as proton motive force and the translocation chaperone SecDFYajC, were omitted. The employed minimalistic approach was essential to discriminate the effect of the lipid-constituting UFAs on SecA recruitment and SecA : SecYEG activity, while maintaining the key physiologically relevant characteristics of the membrane, such as fluidity, the abundance of anionic lipids and the thickness of the hydrophobic core. A follow-up analysis may be conducted in more complex environments, such as membrane extracts and living cells. The demonstrated role of UFAs as mediators of SecA binding and protein translocation may be a critical factor for the reaction in living cells. Bacteria tune their membrane lipid composition in response to environmental factors and growth conditions, so the fraction of mono-UFAs and related cyclopropane-containing fatty acids in mesophilic bacteria, such as *E. coli* and *Pseudomonas aeruginosa*, increases up to 70 mol % at low temperatures [8,9,49]. Our data suggest that the modification of the lipid membrane within this range, as well as the presence of cardiolipins at the physiological concentrations of 5-10 mol %, will favour the membrane-bound state of SecA and thus promote protein transport to compensate for the temperature-dependent kinetics decay. Complementary, under conditions of hyperosmotic shock and increased intracellular salt concentration or dissipation of the proton motive force, the hydrophobic interactions of SecA with unsaturated lipids will prevent dissociation of the ATPase from the membrane. Likewise, it is to expect that SecA homologs from extremophile species are evolutionary tuned for interactions with UFA-depleted membranes, for example via the strong hydrophobic dipole at the N-terminal domain. Comparative functional analysis of SecA homologs from those species, and potentially the reconstituted SecA : SecYEG machinery, may further advance the understanding of the molecular adaptation mechanisms.

Materials and methods

Protein purification

Overexpression of SecYEG with the N-terminal deca-histidine tag in *E. coli* C41(DE3) cells was induced with 0.5 mM IPTG and carried out for 2 h at 37 °C. Cells were harvested by centrifugation and resuspended in buffer R (50 mM KOAc, 20 mM Hepes/KOH pH 7.4, 5 mM $Mg(OAc)_2$, 5% glycerol, 1 mM DTT and cOmplete Protease inhibitor cocktail (Roche, Mannheim, Germany)). Cells were lysed (Microfluidizer, M-110P, Microfluidics Corp., Westwood, MA, USA), and the debris was removed by centrifugation. Crude membranes were pelleted by centrifugation for 1 h at 40 000 r.p.m. (45 Ti rotor, Beckman Coulter, Brea, CA, USA) and then resuspended in buffer R. The membranes were solubilized using 1% DDM in presence of 500 mM KCl, 50 mM Hepes/KOH pH 7.4, 5% glycerol, 200 μM TCEP and the protease inhibitor cocktail. His_{10}-tagged SecYEG was isolated using Ni^{2+}-NTA agarose resin (Qiagen, Hilden, Germany). Once bound to Ni^{2+}-NTA beads, the single-cysteine $SecY^{C148}EG$ variant was optionally labelled with ATTO 643-maleimide (ATTO-Tec GmbH) upon incubation with 100-200 μM dye for 2 h at 4 °C [15]. SecYEG-loaded resin was extensively washed with 50 mM Hepes/KOH pH 7.4, 500 mM KCl, 5% glycerol, 10 mM imidazole, 200 μM TCEP, 0.1% DDM and the protein was eluted with the buffer containing 300 mM imidazole. The protein was transferred to 50 mM Hepes/KOH pH 7.4, 150 mM KCl, 5% glycerol, 0.05% DDM, 200 μM TCEP using PD MidiTrap G-25 column (Cytiva/GE Life Sciences, Freiburg, Germany). Optionally, size-exclusion chromatography (SEC) was carried out using Superdex 200 30/10 GL Increase column (Cytiva/GE Life Sciences) to control the homogeneity of the sample (elution peak at 12.5 mL corresponds to SecYEG in a DDM micelle, total mass of approx. 145 kDa). Protein concentration was determined spectrophotometrically (extinction coefficient 72 000 M^{-1} cm^{-1}). The expression and purification steps were controlled with SDS/PAGE (Quick Coomassie stain, Serva), and in-gel fluorescence of the SecY-conjugated ATTO 643 dye was visualized (Amersham Imager 680RGB, GE Healthcare Life Sciences).

SecA gene was cloned into pET21a plasmid to carry the C-terminal His_6-tag. SecA overexpression in *E. coli* BL21 (DE3) cells was induced with 0.5 mM IPTG and carried out for 2 h at 30 °C. Cells were then harvested by centrifugation and resuspended in 50 mM KOAc, 20 mM Tris/HCL pH 7.5, 5 mM $Mg(OAc)_2$, 20% glycerol, 1 mM DTT and cOmplete protease inhibitor cocktail. Cells were lysed, and the lysate was clarified by centrifugation for 1 h at 100 000 g (45 Ti rotor, Beckman Coulter). The clarified lysate was incubated with Ni^{2+}-NTA agarose resin for 1 h at 4 °C, and the resin was then washed with 500 mM KOAc, 20 mM Tris/HCL pH 7.5, 5 mM $Mg(OAc)_2$, 20% glycerol, 20 mM imidazole and 1 mM DTT. SecA was eluted with the buffer containing 300 mM imidazole. The eluted fractions were concentrated using Amicon Ultra-4 filtering device, cut-off size 50 kDa (Millipore, Darmstadt, Germany) and SecA was subject to SEC using Superose 6 Increase 10/300 GL column (Cytiva/GE Life Sciences) in 50 mM KOAc, 20 mM Tris/HCL pH 7.5, 5 mM $Mg(OAc)_2$,

20% glycerol, 1 mM DTT, resulting in a peak at ~ 15.5 mL elution volume. Peak fractions were pooled together, and the protein concentration was determined spectrophotometrically (extinction coefficient 75 000 M^{-1} cm^{-1}). Precursor proteins proOmpA and proOmpA-DHFR were overexpressed in inclusion bodies as previously described elsewhere [50,51] and stored in 8 M urea.

Liposomes preparation

Synthetic lipids and *E. coli* polar lipid extract were purchased from Avanti Polar Lipids, Inc. as stocks in chloroform. The lipids were mixed in desired ratios, and chloroform was evaporated under vacuum conditions at 40 °C using a rotary evaporator (IKA). The dried lipid film was then rehydrated in 50 mM KCl, 50 mM Hepes/KOH pH 7.4 to achieve the lipid concentration of 5 mM. To form large unilamellar vesicles, the crude liposomes were manually extruded through the porous polycarbonate membranes (Nuclepore, Whatman) using the Mini-Extruder set (Avanti Polar Lipids, Inc.). The membrane pore size was decreased stepwise from 400 nm to 200 nm, and vesicle sizes were controlled by dynamic light scattering (Nicomp 3000, Entegris, Inc., Billerica, MA, USA).

SecYEG reconstitution

SecYEG variants were reconstituted in liposomes with different composition at 1 : 1000 protein : lipid ratio as follows. Liposomes were swelled by adding 0.2% DDM followed by incubation for 10 min at 40 °C and then mixed with SecYEG in 0.05% DDM. The reconstitution mixture was incubated for 30 min on ice. The detergent was then removed upon incubation with Bio-Beads SM-2 sorbent (Bio-Rad Laboratories, Feldkirchen, Germany) overnight at 4 °C. Formed proteoliposomes were pelleted upon centrifugation at 80 000 r.p.m. for 30 min (S120-AT3 rotor, Thermo Fisher/Sorvall) and resuspended in 50 mM KCl, 50 mM Hepes/KOH pH 7.4 to achieve the final translocon concentration of 5 μM. To examine the reconstitution efficiency, the proteoliposomes were subjected to centrifugation in the density gradient. 100 μL of proteoliposomes were diluted and mixed with 54% iodixanol-based medium (Optiprep™, Merck/Sigma) to achieve the final iodixanol concentration of 40%. 30% iodixanol was then layered on top followed by 15% and 5%. Samples were centrifuged for 3 h at 200 000 g (TST 60.4 swing-out rotor, Thermo Fisher/Sorvall). The gradients were manually fractionated, and the contents were precipitated with trichloroacetic acid (TCA) and analysed on SDS/PAGE.

SecYEG topology in the formed proteoliposomes was analysed by probing the accessibility of the SecY cytoplasmic side. The recombinant SecYEG bears the N-terminal histidine tag on SecY subunit followed by an enterokinase cleavage site [5]. By cleaving the tag from SecYEG reconstituted in liposomes, the amount of correctly oriented SecYEG could be determined due to difference in migration on SDS/PAGE. 5 μL proteoliposomes were mixed with 8 units of enterokinase light chain (New England Biolabs) and diluted to 20 μL, then samples were incubated at 25 °C overnight.

Reconstitution of SecYEG into MSP2N2 nanodiscs was carried out following the previously established protocol [6,34,36]. To achieve the monomeric state of the translocon, a large excess of lipids and the scaffold protein MSP was supplied into the reconstitution reaction (SecYEG : MSP : lipid ratio of 1 : 10 : 1000). SecYEG-loaded and empty nanodiscs were separated via size exclusion chromatography using Superdex 200 10/300 Increase GL column (Cytiva/GE Life Sciences).

In vitro translocation assay

The previously described protocol for the fluorescently labelled preprotein translocation *in vitro* was followed with minor modifications [15,52]. 10 μL of proteoliposomes was mixed with 1 μM SecA (concentration for monomer), 0.5 μM SecB (concentration for tetramer), energy mix (0.05 $mg{\cdot}mL^{-1}$ phosphocreatine kinase, 10 mM phosphocreatine), 0.1 $mg{\cdot}mL^{-1}$ BSA, 10 mM DTT, 10 mM $MgCl_2$ and 1 μM proOmpA labelled with fluorescein-maleimide (proOmpA-FM). The total volume was adjusted to 50 μL with buffer (50 mM KCl, 50 mM Hepes/KOH pH 7.4), and samples were equilibrated at 37 °C for 5 min. The translocation was triggered by the addition of 6 mM ATP and left to proceed for 15 min. Afterwards, 10% volume was withdrawn as a reference for the input of proOmpA-FM, and 0.2 $mg{\cdot}mL^{-1}$ proteinase K was added to the remaining sample to degrade the nontranslocated preprotein. After incubation for 15 min, 150 μL 20% TCA was added, and the aggregated samples were pelleted via centrifugation at 20 000 g for 10 min (Eppendorf 5417 R table-top centrifuge). The pellets were washed with 500 μL ice-cold acetone and centrifuged for 5 min. Acetone was discarded, and the dried pellets were resuspended in 15 μL 2.5x SDS/PAGE sample buffer, incubated for 5 min at 95 °C and then loaded on SDS/PAGE. In-gel fluorescence of the protease-protected proOmpA-FM was recorded and quantified (IMAGEQUANT TL, Cytiva/GE Life Sciences). The background signal was subtracted using the implemented Local average algorithm. The amount of the transported proOmpA-FM was determined based on the available reference sample. At least two independent tests were carried out for each experiment.

FRET-based real-time kinetics assay

FRET-based analysis of the preprotein translocation was carried out following the previously established protocol [15,26]. Briefly, $proOmpA^{C292}$-DHFR fusion protein was labelled with Cyanine3-maleimide (donor) at the unique cysteine at position 292 of proOmpA domain, and $SecY^{C148}EG$ was labelled with ATTO 643-maleimide

(acceptor) at the periplasmic side. To record the acceptor fluorescence, the monochromators of the thermostated spectrofluorometer (Fluorolog-3, Horiba™ Scientific) were set to the excitation wavelength of 510 nm (slit width 3 nm) and the emission wavelength of 690 nm (3 nm slit width). Prior the translocation, the DHFR domain was stably folded in presence of the cofactors methotrexate and NADPH, as previously described [15]. 100 nM proOmpA-DHFR was mixed with 5 μL proteoliposomes (400 nM SecYEG, dual orientation) in presence of 1 μM SecA and completed to 60 μL of buffer (150 mM KCl, 5 mM $MgCl_2$, 50 mM Hepes/KOH pH 7.4). The quartz cuvette (Hellma Analytics) was incubated at 37 °C for 150 s, and the translocation reaction was triggered by the addition of 5 mM ATP. The acceptor fluorescence was recorded for 20 min. Rate constants for FRET-dependent fluorescence were extracted using Origin software by fitting the curves to a one-phase association exponential function:

$$Y = Y_b + A\left(1 - e^{-kt}\right) \quad \text{Eq (1).}$$

where Y_b is baseline, A is the amplitude, k is the rate constant, and t is time. At least two independent tests were carried out for each experiment.

ATPase assay

SecA ATPase activity assay was done using malachite green kit (MAK307, Merck/Sigma, Darmstadt, Germany). Briefly, 25 nM or 0.5 μM SecA was mixed with 0.5 μM SecB, 1 μM proOmpA and 10 mM DTT, 5 mM $MgCl_2$ in the presence of 50 mM Hepes/KOH pH 7.4 and 150 mM KCl. 0.125 or 1 mM SecYEG proteoliposomes (or 1 μM SecYEG) were added; the reaction was started by the addition of ATP and incubated for 15 or 30 min at 37 °C. The reaction was diluted 10 times when necessary. Afterwards, the reaction was stopped by the addition of 20 μL working reagent supplied with the kit. The colour was allowed to develop for 30 min at the ambient temperature, and the absorbance was measured at 590 nm. The data were fitted to Michaelis–Menten equation:

$$V = V_{\max} \frac{[S]}{K_m + [S]} \quad \text{Eq (2).}$$

where V is the reaction velocity, $V_{\max}$ is the maximum reaction velocity, [S] is the ATP concentration, and K_m is the Michaelis's constant. At least two independent tests were carried out for each experiment.

SecA flotation assay

SecA was mixed with liposomes in protein : lipid molar ratio of 1 : 5000, and the volume was completed to 100 μL with the buffer (50 mM KCl, 50 mM Hepes/KOH pH 7.4, 5 mM $MgCl_2$). When mentioned, elevated concentrations of KCl were used. Samples were incubated 30 min at 25 °C and then mixed with 60% sucrose (w/v) to achieve final sucrose concentration of 30%. The samples were loaded in the centrifugation tube (S12-AT3 rotor, Thermo Fisher/Sorvall), followed by 20% sucrose solution (250 μL) and the sucrose-free buffer (50 μL). Samples were centrifuged for 1 h at 80 000 r.p.m. (AT3 rotor). Samples were then fractionated into 3 fractions, top (125 μL), middle (125 μL) and bottom (250 μL), and then precipitated by the addition of 200 μL of 20% TCA. The pellets were resuspended in the sample buffer and loaded on SDS/PAGE. The intensity of Coomassie-stained bands was quantified (IMAGEQUANT TL, Cytiva/GE Life Sciences), and the amount of SecA bound to liposomes was determined by dividing the intensity of the floating fraction (top) by the integral intensity of all fractions. At least two independent tests were carried out for each experiment.

Surface Plasmon resonance

SecA : lipid binding experiments were performed using L1 sensor chip on two-channel Biacore X100 instrument (GE Healthcare Life Sciences). SPR relies on changes in the evanescence wave within a short distance, typically ~ 100 nm, above the sensor surface, so the liposomes were additionally pre-extruded to the diameter of 50 nm. Prior the experiment, the chip surface was cleaned with 20 mM CHAPS (2 injections for 30 s each) and conditioned using SPR running buffer (150 mM KCl, 5 mM $MgCl_2$, 50 mM Hepes/KOH pH 7,4). The unilamellar liposomes were immobilized at the flow rate of 5 μL·min^{-1} for 600 s to achieve 7000 to 10 000 response units. DOPC-only liposomes lacking SecA interaction were immobilized in the reference channel. Afterwards, 2 injections of 100 mM NaOH were performed to remove loosely attached material. SecA was transferred into the SPR running buffer and was injected for 150 s at the flow rate of 10 μL·min^{-1}. When indicated, 300 mM KCl was used instead of 150 mM KCl in SPR running buffer to probe SecA binding at higher ionic strength. After each measurement, the chip surface was regenerated (2 injections of 20 mM CHAPS), so the immobilized liposomes were removed. Data were fitted by nonlinear regression analysis of response levels at the steady state to one-site binding model:

$$Req = \frac{KaCR_{\max}}{KaC+1} + offset \quad \text{Eq (3).}$$

where Ka is the association constant, C is the concentration of SecA, R_{max} is the maximum response unit, and offset is the intercept of the fitted curve on the y-axis. Due to extensive binding of SecA to liposome surfaces and potential dissociation/re-binding events known as mass transfer effect, a detailed analysis on binding/dissociation kinetics was omitted. Notably, though, the binding/dissociation recordings were not altered upon increasing the flow rate to 30 μL·min^{-1}, as would be expected under the conditions of the mass transfer effect.

Quartz crystal microbalance

Quartz crystal microbalance (QCM) measurements were carried using Q-Sense Omega Auto instrument (Biolin Scientific, Gothenburg, Sweden). This technique allows the real-time monitoring of SecA interactions with planar supported lipid bilayers (SLBs) by measuring the shifts in the resonance frequency and dissipation energy, which proportionally depend on the mass changes and changes in viscoelastic properties on the surface of the chip, respectively. The formation of SLBs on the QCM-D sensor chip (QSX 303 SiO_2) was performed as follows. The surface of the plasma-treated sensor chip was equilibrated with aqueous buffer (50 mM Tris/HCL pH 7.4, 150 mM KCl) for 3 min to stabilize the frequency and dissipation energy baselines. Freshly extruded liposome suspension (extrusion via 100 nm membrane) was injected over the chip surface at flow rate of 50 $\mu L \cdot min^{-1}$ for 5 min in 50 mM Tris/HCl pH 7.4, 150 mM KCl, 10 mM $CaCl_2$. The liposomes could adsorb on the chip surface and underwent spontaneous collapse, which resulted in formation of SLBs. To remove loosely bound material from the chip surface, the surface was subsequently washed with the buffer (50 mM Tris/HCL pH 7.4 and 150 mM KCl). SLB formation resulted in a frequency shift of -27 ± 1 Hz and the energy dissipation of 0.7 ± 0.1, which is in excellent agreement with previously published data [53]. To probe SecA interaction with the SLBs, the ATPase was transferred into the running buffer (50 mM Tris/HCL pH 7.4, 150 mM KCl, 5 mM $MgCl_2$) and the protein solution was then injected over the SLBs at flow rate of 50 $\mu L \cdot min^{-1}$. To determine the affinity of SecA to lipids, the concentration of the ATPase was varied in dilution series from 40 nM to 5.25 μM concentration, and the maximum change in the chip oscillation frequency was measured. Prior each cycle, the surface of the SLB was washed with the high-salt buffer (1 M NaCl, 20 mM Tris/HCL pH 7.4) and then with the running buffer to remove the bound SecA and equilibrate the SLB surface for the next round. The equilibrium dissociation constant (K_d) for this measurement was determined by plotting steady-state net-frequency signal responses prior to dissociation phase (R_{max}) against the corresponding SecA concentration (C). Data were fitted using GraphPad Prism 9 based on one-site binding model:

$$R_{eq} = \frac{R_{max} * C}{K_d + C} \quad \text{Eq (4).}$$

Membrane fluidity analysis

Liposomes were mixed with 0.1 μM 1,6-diphenyl-1,3,5-hexatriene (DPH) to achieve dye : lipid ratio of 1 : 1000. Samples were incubated for 1 h at 25 °C in the dark. DPH fluorescence was recorded at 428 nm (slit width 5 nm) with the excitation wavelength of 350 nm (slit width 5 nm) using Fluorolog-3 fluorometer. Steady-state anisotropy (r) was calculated as:

$$r = \frac{I_{vv} - G I_{vh}}{I_{vv} + 2 G I_{vh}} \quad \text{Eq (5).}$$

where I is the fluorescence intensity, and v and h denote the vertical and horizontal setting for the excitation and emission polarizers, respectively, G is the instrumental correction factor which is provided by the instrument for each measurement. At least two independent tests were carried out for each experiment.

Lipid packing analysis

Liposomes (lipid concentration 100 μM) were mixed with 0.3 μM laurdan to achieve dye : lipid ratio of 1 : 333. Samples were incubated at 37 °C for 1 h in the dark in presence of 50 mM KCl, 5 mM $MgCl_2$, 50 mM Hepes/KOH pH 7.4. Laurdan emission spectrum was recorded from 400 to 600 nm (slit width 3 nm) with the excitation wavelength of 350 nm (slit width 3 nm) using Fluorolog-3 fluorometer. Generalized polarization value (GP) was calculated as a ratio of integrated intensities from 400 nm to 460 nm (I_1) and from 470 nm to 550 nm (I_2):

$$GP = \frac{I1 - I2}{I1 + I2} \quad \text{Eq (6).}$$

At least two independent tests were carried out for each experiment.

Cardiolipin head group parametrization

The parameters for the cardiolipin head group were obtained following the linings established in Lipid11 [54] and Lipid14 [55]. Briefly, multiple conformations of the methyl-capped headgroup were generated with Balloon, using an RMSD cutoff of 1 Å. The resulting 21 independent structures were optimized, and the electrostatic potential (ESP) was computed, using Gaussian 09 at the HF/6-31G* theory level, with parameters as given by antechamber [56]. The resulting ESP for all conformations was combined into a multiconformational fit, fixing the capping methyl group charges as established in Lipid11 [54] and using a standard two-step RESP procedure [56]. The obtained partial atomic charges were used together with Lipid17 atom types to generate an AMBER force field library file with LEaP. As the head group has four positions where acyl chains have to be attached (compared to the standard two attachment points per residue in AMBER), explicit bonds have to be set for two positions per cardiolipin when parametrizing a membrane system in LEaP. The parameters have been included in PACKMOL-Memgen [57] of AMBER20, where all combinations of the headgroup with every possible acyl chain in Lipid17 have been considered.

MD simulations

Systems for molecular dynamics simulations were prepared with PACKMOL-Memgen [57], using a length of the

membrane in x and y direction of 100 Å and default options otherwise. To mimic the experimental conditions, compositions of DOPC : DOPG 70 : 30, POPC : POPG 70 : 30, POPC : bis(PO)CL 85 : 15 and POPC : TOCL 85 : 15 were prepared. In addition, systems of DOPC : DOPG 70 : 30 and POPC : POPG 70 : 30 including the 25 N-terminal residues of SecA with an N-methyl amide cap in the C terminus at 25 Å of the membrane surface were prepared. The peptide structure was modelled with TopModel [58], using as main templates *E. coli* SecA (PDB ID : 3BXZ) and *B. subtilis* SecA (PDB ID : 3DL8). In all cases, potassium ions were added to neutralize the charges introduced by the negatively charged headgroups. To ensure independent starting configurations, all systems were packed five times with a different random seed.

From the packed systems, independent replicas were energy-minimized using the pmemd implementation included in AMBER18 [59], using ff14SB [60], TIP3P [61] and Lipid17 [55,62] parameters for the protein, water and membrane lipids, respectively. To relax the system stepwise, alternating steepest descent/conjugate gradient energy minimizations with a maximum of 20 000 steps each were performed. Initially, the positions of the membrane were restrained during minimization; the final round of minimization was performed without restraints. To thermalize the systems, a Langevin thermostat [63] with a friction coefficient of 1 ps^{-1} was used. The pressure, when required, was maintained using a semi-isotropic Berendsen barostat [64] with a relaxation time of 1 ps, coupling the membrane (xy) plane. The system was heated by gradually increasing the temperature from 10 to 100 K for 5 ps under NVT conditions, and from 100 to 300 K for 115 ps under NPT conditions at 1 bar. The thermalization process was continued for 5 ns under NPT conditions, after which production runs of 1 µs length were performed using the same conditions with the pmemd GPU implementation [65], constraining covalent bonds to hydrogens with the SHAKE algorithm [66] and using a time step of 2 fs.

The trajectories were analysed with cpptraj [67] as to lipid order parameters and electron density profiles. The lipid order parameter describes the level of order imposed on the lipid molecules in a bilayer arrangement and relates with deuterium-NMR measurements [68]. The electron density profile describes the probability of finding electron-rich regions along the membrane normal and can be related to X-ray scattering experiments [69]. As the membrane has an anisotropic, that is planar arrangement, it gives information regarding the bilayer arrangement, which in simulations can be additionally decomposed according to the contribution of each system component, obtaining information of its location along the membrane normal. In all cases, the profiles describe well-behaved membrane bilayers. The contacts of the SecA N-terminal peptide with the membrane headgroups were evaluated as the sum of the per-residue contributions as obtained from the native contacts routine, using a cut-off of 4.5 Å. The average area per lipid of each system was calculate with cpptraj from the area of the xy plane and the number of lipids on each leaflet. To measure the per-lipid type contribution to the area per lipid, the APL@Voro software was used [70]. For this, the trajectories were centred and imaged on the bilayer, and transformed into the GROMACS XTC format with cpptraj. Afterwards, the trajectories were processed with the software, assigning the phosphorous atoms (or the central carbon of the glycerol moiety of cardiolipins) to the area by tessellation. The average xz particle density was calculated using the volmap function of cpptraj, which represents each atom as a Gaussian with a standard deviation equal to the atomic radius, similarly to what has been described previously [11]. Briefly, a 80x80x80 Å grid centred in the membrane centre, with a 1 Å spacing in every dimension, and the average density was calculated along the 1 µs simulation of each system. To obtain the xz profile, the density along the y dimension was averaged.

To calculate the lateral pressure of the equilibrated systems after 1 µs of simulation time as a function of the z-coordinate, all replicas were extended for additional 100 ns, recording the coordinates and velocities every 5 ps. The obtained trajectory was centred on the bilayer, transformed to GROMACS TRR format with cpptraj and postprocessed with GROMACS-LS to obtain the stress tensors [71]. For this, a nonbonded cut-off of 20 Å and otherwise equivalent conditions to the production run were used, processing each ns of simulation independently and calculating the average stress tensor with the provided tensortools script. The lateral pressure was calculated according to equation Eq. 7

$$\Pi(z) = \frac{P_{xx}(z)+P_{yy}(z)}{2} - P_N(z) \qquad \text{Eq (7).}$$

where the first term corresponds to the average lateral term (P_L), and P_N corresponds to the normal component.

Acknowledgements

We thank Alexander Büll and Nicola Vettore (DTU Denmark) for the assistance with the QCM experiments. The research was supported by the Deutsche Forschungsgemeinschaft (DFG) via the research grant KE1879/3-1 to AK and projects A10 (AK) and A03 (HG) within the CRC 1208. We are grateful for computational support and infrastructure provided by the 'Zentrum für Informations- und Medientechnologie' (ZIM) at the Heinrich Heine University Düsseldorf and the computing time provided by the John von Neumann Institute for Computing (NIC) to H.G. on the supercomputer JURECA at Jülich Supercomputing Centre (JSC, user IDs: plaf and HKF7). Open Access funding enabled and organized by Projekt DEAL.

Conflict of interest

The authors declare no conflict of interest in relation to the presented work.

Author contributions

MK performed biochemical and fluorescence-based analysis; MK and ML carried out SPR and DSF measurements; ML carried out QCM experiments; MK, ML and AK analysed and interpreted the data; SSV and HG carried out the computational simulations and interpreted the data in cooperation with MK and AK; all authors contributed to writing and editing the manuscript.

References

1 Tsirigotaki A, De Geyter J, Šoštarić N, Economou A & Karamanou S (2017) Protein export through the bacterial Sec pathway. *Nat Rev Microbiol* **15**, 21–36.
2 Kusters I & Driessen AJM (2011) SecA, a remarkable nanomachine. *Cell Mol Life Sci* **68**, 2053–2066.
3 Breukink E, Demel RA, de Korte-Kool G & de Kruijff B (1992) SecA insertion into phospholipids is stimulated by negatively charged lipids and inhibited by ATP: A monolayer study. *Biochemistry* **31**, 1119–1124.
4 Wu ZC, De Keyzer J, Kedrov A & Driessen AJM (2012) Competitive binding of the SecA ATPase and ribosomes to the SecYEG translocon. *J Biol Chem* **287**, 7885–7895.
5 Van Der Does C, Swaving J, Van Klompenburg W & Driessen AJM (2000) Non-bilayer lipids stimulate the activity of the reconstituted bacterial protein translocase. *J Biol Chem* **275**, 2472–2478.
6 Kater L, Frieg B, Berninghausen O, Gohlke H, Beckmann R & Kedrov A (2019) Partially inserted nascent chain unzips the lateral gate of the Sec translocon. *EMBO Rep* **20**, e48191.
7 Koch S, Exterkate M, López CA, Patro M, Marrink SJ & Driessen AJM (2019) Two distinct anionic phospholipid-dependent events involved in SecA-mediated protein translocation. *Biochim Biophys Acta - Biomembr* **1861**, 183035.
8 Morein S, Andersson A & Rilfors L (1996) Wild-type Escherichia coli cells regulate the membrane lipid composition in a "window" between gel and non-lamellar structures. *J Biol Chem* **271**, 6801–6809.
9 Siliakus MF, van der Oost J & Kengen SWM (2017) Adaptations of archaeal and bacterial membranes to variations in temperature, pH and pressure. *Extremophiles* **21**, 651–670.
10 Vanni S, Hirose H, Gautier R & Antonny B (2014) A sub-nanometre view of how membrane curvature and composition modulate lipid packing and protein recruitment. *Nat Commun* **5**, 4916.
11 Ballweg S, Sezgin E, Doktorova M, Covino R, Reinhard J, Wunnicke D, Hänelt I, Levental I, Hummer G & Ernst R (2020) Regulation of lipid saturation without sensing membrane fluidity. *Nat Commun* **11**, e756.
12 Drin G & Antonny B (2010) Amphipathic helices and membrane curvature. *FEBS Lett* **584**, 1840–1847.
13 Sohlenkamp C & Geiger O (2016) Bacterial membrane lipids: Diversity in structures and pathways. *FEMS Microbiol Rev* **40**, 133–159.
14 Lentz BR (1989) Membrane "fluidity" as detected by diphenylhexatriene probes. *Chem Phys Lipids* **50**, 171–190.
15 Kedrov A, Kusters I, Krasnikov VV & Driessen AJM (2011) A single copy of SecYEG is sufficient for preprotein translocation. *EMBO J* **30**, 4387–4397.
16 Roussel G, Lindner E & White SH (2019) Stabilization of SecA ATPase by the primary cytoplasmic salt of Escherichia coli. *Protein Sci* **28**, 984–989.
17 Prabudiansyah I, Kusters I, Caforio A & Driessen AJM (2015) Characterization of the annular lipid shell of the Sec translocon. *Biochim Biophys Acta - Biomembr* **1848**, 2050–2056.
18 Corey RA, Pyle E, Allen WJ, Watkins DW, Casiraghi M, Miroux B, Arechaga I, Politis A & Collinson I (2018) Specific cardiolipin–SecY interactions are required for proton-motive force stimulation of protein secretion. *Proc Natl Acad Sci* **115**, 7967–7972.
19 Koch S, Seinen A-B, Kamel M, Kuckla D, Monzel C, Kedrov A & Driessen AJM (2021) Single-molecule analysis of dynamics and interactions of the SecYEG translocon. *FEBS J* **288**, 2203–2221.
20 Kotov V, Bartels K, Veith K, Josts I, Subhramanyam UKT, Günther C, Labahn J, Marlovits TC, Moraes I, Tidow H *et al.* (2019) High-throughput stability screening for detergent-solubilized membrane proteins. *Sci Rep* **9**, 10379.
21 De Keyzer J, Van der Does C, Swaving J & Driessen AJM (2002) The F286Y mutation of PrlA4 tempers the signal sequence suppressor phenotype by reducing the SecA binding affinity. *FEBS Lett* **510**, 17–21.
22 Harris FM, Best KB & Bell JD (2002) Use of laurdan fluorescence intensity and polarization to distinguish between changes in membrane fluidity and phospholipid order. *Biochim Biophys Acta - Biomembr* **1565**, 123–128.
23 Cantor RS (1999) Lipid composition and the lateral pressure profile in bilayers. *Biophys J* **76**, 2625–2639.
24 Ollila OHS & Vattulainen I (2010) Lateral Pressure Profiles in Lipid Membranes: Dependence on Molecular Composition. Molecular Simulations and Biomembranes: From Biophysics to Function, pp. 26–55. The Royal Society of Chemistry.

25 Findik BT, Smith VF & Randall LL (2018) Penetration into membrane of amino- terminal region of SecA when associated with SecYEG in active complexes. *Protein Sci* **27**, 681–691.
26 Koch S, De Wit JG, Vos I, Birkner JP, Gordiichuk P, Herrmann A, Van Oijen AM & Driessen AJM (2016) Lipids activate SecA for high affinity binding to the SecYEG complex. *J Biol Chem* **291**, 22534–22543.
27 Jilaveanu LB, Zito CR & Oliver D (2005) Dimeric SecA is essential for protein translocation. *Proc Natl Acad Sci USA* **102**, 7511–7516.
28 Bauer BW, Shemesh T, Chen Y & Rapoport TA (2014) A "push and slide" mechanism allows sequence-insensitive translocation of secretory proteins by the SecA ATPase. *Cell* **157**, 1416–1429.
29 Cabelli RJ, Dolan KM, Qian L & Oliver DB (1991) Characterization of membrane-associated and soluble states of SecA protein from wild-type and secA51(Ts) mutant strains of *Escherichia coli*. *J Biol Chem* **266**, 24420–24427.
30 Seinen A-B, Spakman D, van Oijen AM & Driessen AJM (2021) Cellular dynamics of the SecA ATPase at the single molecule level. *Sci Rep* **11**, 1433.
31 Nielsen SB & Otzen DE (2019) Quartz crystal microbalances as tools for probing protein-membrane interactions. *Methods Mol Biol* **2003**, 31–52.
32 Park E & Rapoport TA (2012) Bacterial protein translocation requires only one copy of the SecY complex in vivo. *J Cell Biol* **198**, 881–893.
33 Ryabichko S, Ferreira VDM, Heidi V, Kiyamova R, Dowhan W & Bogdanov M (2020) Cardiolipin is required in vivo for the stability of bacterial translocon and optimal membrane protein translocation and insertion. *Sci Rep* **10**, 6296.
34 Taufik I, Kedrov A, Exterkate M & Driessen AJM (2013) Monitoring the activity of single translocons. *J Mol Biol* **425**, 4145–4153.
35 Koch S, Driessen AJM & Kedrov A (2018) Biophysical analysis of sec-mediated protein translocation in nanodiscs. *Adv Biomembr Lipid Self-Assembly* **28**, 41–85.
36 Ritchie TK, Grinkova YV, Bayburt TH, Denisov IG, Zolnerciks JK, Atkins WM & Sligar SG (2009) Reconstitution of membrane proteins in phospholipid bilayer nanodiscs. *Methods Enzymol* **464**, 211–231.
37 Harayama T & Riezman H (2018) Understanding the diversity of membrane lipid composition. *Nat Rev Mol Cell Biol* **19**, 281–296.
38 Strahl H & Errington J (2017) Bacterial membranes : structure, domains, and function. *Annu Rev Microbiol* **71**, 519–538.
39 Das S, Stivison E, Folta-Stogniew E & Oliver D (2008) Reexamination of the role of the amino terminus of SecA in promoting its dimerization and functional state. *J Bacteriol* **190**, 7302–7307.
40 Roussel G & White SH (2020) Binding of SecA ATPase monomers and dimers to lipid vesicles. *Biochim Biophys Acta - Biomembr* **1862**, 183112.
41 Matin TR, Sigdel KP, Utjesanovic M, Marsh BP, Gallazzi F, Smith VF, Kosztin I & King GM (2017) Single-molecule peptide–lipid affinity assay reveals interplay between solution structure and partitioning. *Langmuir* **33**, 4057–4065.
42 Kusters I, Van Den Bogaart G, Kedrov A, Krasnikov VV, Fulyani F, Poolman B & Driessen AJM (2011) Quaternary structure of SecA in solution and bound to SecYEG probed at the single molecule level. *Structure* **19**, 430–439.
43 Sardis MF & Economou A (2010) SecA: A tale of two protomers: MicroReview. *Mol Microbiol* **76**, 1070–1081.
44 Gold VAM, Robson A, Bao H, Romantsov T, Duong F & Collinson I (2010) The action of cardiolipin on the bacterial translocon. *Proc Natl Acad Sci* **107**, 10044–10049.
45 Roussel G & White SH (2020) The SecA ATPase motor protein binds to Escherichia coli liposomes only as monomers. *Biochim Biophys Acta - Biomembr* **1862**, 183358.
46 Gold VAM, Robson A, Clarke AR & Collinson I (2007) Allosteric regulation of SecA: Magnesium-mediated control of conformation and activity. *J Biol Chem* **282**, 17424–17432.
47 Deville K, Gold VAM, Robson A, Whitehouse S, Sessions RB, Baldwin SA, Radford SE & Collinson I (2011) The oligomeric state and arrangement of the active bacterial translocon. *J Biol Chem* **286**, 4659–4669.
48 Unsay JD, Cosentino K, Subburaj Y & García-Sáez AJ (2013) Cardiolipin effects on membrane structure and dynamics. *Langmuir* **29**, 15878–15887.
49 Kropinski AMB, Lewis V & Berry D (1987) Effect of growth temperature on the lipids, outer membrane proteins, and lipopolysaccharides of Pseudomonas aeruginosa PAO. *J Bacteriol* **169**, 1960–1966.
50 Kusters I, van den Bogaart G, de Wit J, Krasnikov V, Poolman B & Driessen A (2010) Purification and Functional Reconstitution of the Bacterial Protein Translocation Pore, the SecYEG Complex. *Methods Mol Biol* **619**, 131–143.
51 Bol R, De Wit JG & Driessen AJM (2007) The active protein-conducting channel of Escherichia coli contains an apolar patch. *J Biol Chem* **282**, 29785–29793.
52 De Keyzer J, Van der Does C & Driessen AJM (2002) Kinetic analysis of the translocation of fluorescent precursor proteins into Escherichia coli membrane vesicles. *J Biol Chem* **277**, 46059–46065.
53 Wang L, Biswas KH, Yoon BK, Kawakami LM, Park S, Groves JT, Li L, Huang W & Cho N-J (2018) Membrane reconstitution of monoamine oxidase

enzymes on supported lipid bilayers. *Langmuir* **34**, 10764–10773.
54 Skjevik ÅA, Madej BD, Walker RC & Teigen K (2012) LIPID11: a modular framework for lipid simulations using amber. *J Phys Chem B* **116**, 11124–11136.
55 Dickson CJ, Madej BD, Skjevik ÅA, Betz RM, Teigen K, Gould IR & Walker RC (2014) Lipid14: the amber lipid force field. *J Chem Theory Comput* **10**, 865–879.
56 Wang J, Wang W, Kollman PA & Case DA (2006) Automatic atom type and bond type perception in molecular mechanical calculations. *J Mol Graph Model* **25**, 247–260.
57 Schott-Verdugo S & Gohlke H (2019) PACKMOL-Memgen: A simple-to-use, generalized workflow for membrane-protein–lipid-bilayer system building. *J Chem Inf Model* **59**, 2522–2528.
58 Mulnaes D, Porta N, Clemens R, Apanasenko I, Reiners J, Gremer L, Neudecker P, Smits SHJ & Gohlke H (2020) TopModel: template-based protein structure prediction at low sequence identity using top-down consensus and deep neural networks. *J Chem Theory Comput* **16**, 1953–1967.
59 Darden T, York DM & Pedersen LG (1993) Particle mesh Ewald: An N*log(N) method for Ewald sums in large systems. *J Chem Phys* **98**, 10089–10092.
60 Maier JA, Martinez C, Kasavajhala K, Wickstrom L, Hauser KE & Simmerling C (2015) ff14SB: Improving the Accuracy of Protein Side Chain and Backbone Parameters from ff99SB. *J Chem Theory Comput* **11**, 3696–3713.
61 Jorgensen WL, Chandrasekhar J, Madura JD, Impey RW & Klein ML (1983) Comparison of simple potential functions for simulating liquid water. *J Chem Phys* **79**, 926–935.
62 Case DA, Cerutti DS, Cheatham TE III, Darden TA, Duke RE, Giese TJ, Gohlke H, Goetz AW, Greene D, Homeyer N *et al.* (2017) Amber17. University of California San Francisco.
63 Quigley D & Probert MI (2004) Langevin dynamics in constant pressure extended systems. *J Chem Phys* **120**, 11432.
64 Berendsen HJC, Postma JPM, van Gunsteren WF, Di Nola A & Haak JR (1984) Molecular dynamics with coupling to an external bath. *J Chem Phys* **81**, 3684–3690.
65 Le Grand S, Götz AW & Walker RC (2013) SPFP: Speed without compromise—A mixed precision model for GPU accelerated molecular dynamics simulations. *Comput Phys Commun* **184**, 374–380.
66 Ryckaert J-P, Ciccotti G & Berendsen HJC (1977) Numerical integration of the cartesian equations of motion of a system with constraints: molecular dynamics of n-alkanes. *J Comput Phys* **23**, 327–341.
67 Roe DR & Cheatham TE III (2013) PTRAJ and CPPTRAJ: Software for Processing and Analysis of Molecular Dynamics Trajectory Data. *J Chem Theory Comput* **9**, 3084–3095.
68 Piggot TJ, Allison JR, Sessions RB & Essex JW (2017) On the Calculation of acyl chain order parameters from lipid simulations. *J Chem Theory Comput* **13**, 5683–5696.
69 Liu Y & Nagle JF (2004) Diffuse scattering provides material parameters and electron density profiles of biomembranes. *Phys Rev E* **69**, 40901.
70 Lukat G, Krüger J & Sommer B (2013) APL@Voro: a voronoi-based membrane analysis tool for GROMACS trajectories. *J Chem Inf Model* **53**, 2908–2925.
71 Vanegas JM, Torres-Sánchez A & Arroyo M (2014) Importance of force decomposition for local stress calculations in biomembrane molecular simulations. *J Chem Theory Comput* **10**, 691–702.